

Multiscale Sparse Microcanonical Models

Joan Bruna^{1,2} and Stéphane Mallat^{3,4}

¹Courant Institute of Mathematical Sciences, New York University

²Center for Data Science, New York University

³College de France

⁴Ecole Normale Supérieure, PSL, Paris

June 13, 2022

Abstract

We study density estimation of stationary processes defined over an infinite grid from a single, finite realization. Gaussian Processes and Markov Random Fields avoid the curse of dimensionality by focusing on low-order and localized potentials respectively, but its application to complex datasets is limited by their inability to capture singularities and long-range interactions, and their expensive inference and learning respectively. These are instances of Gibbs models, defined as maximum entropy distributions under moment constraints determined by an energy vector. The Boltzmann equivalence principle states that under appropriate ergodicity, such *macrocanonical* models are approximated by their *microcanonical* counterparts, which replace the expectation by the sample average. Microcanonical models are appealing since they avoid computing expensive Lagrange multipliers to meet the constraints. This paper introduces microcanonical measures whose energy vector is given by a wavelet scattering transform, built by cascading wavelet decompositions and point-wise nonlinearities. We study asymptotic properties of generic microcanonical measures, which reveal the fundamental role of the differential structure of the energy vector in controlling e.g. the entropy rate. Gradient information is also used to define a microcanonical sampling algorithm, for which we provide convergence analysis to the microcanonical measure. Wavelet transforms capture local regularity at different scales, whereas scattering transforms provide scale interaction information, critical to restore the geometry of many physical phenomena. We demonstrate the efficiency of sparse multiscale microcanonical measures on several processes and real data exhibiting long-range interactions, such as Ising, Cox Processes and image and audio textures.

1 Introduction

Building probabilistic models of large systems of interacting variables that can be efficiently estimated from data is a core problem in Statistical Physics, Machine Learning

and Signal Processing. We consider the estimation of the probability measure of stationary processes $X(u)$ on the infinite grid $u \in \mathbb{Z}^\ell$ given a single realization, observed over a finite domain $\Lambda_d \subset \mathbb{Z}^\ell$ of cardinal d . For instance, in image ($\ell = 2$) and audio ($\ell = 1$) texture synthesis, given a piece of texture over Λ_d , one attempts to synthesize similar texture examples by sampling the resulting probability model. Building probability models from a single observation is also needed in finance and in many physical problems, such as geophysics exploration or fluid dynamics. These estimations rely on the ability to build low-dimensional approximations of the underlying stationary measure, with an error which converges to zero when the domain size d goes to ∞ . This paper introduces microcanonical sparse multiscale models, which can take into account non-Gaussian phenomena and long range interactions.

A Gaussian stationary model reduces the estimation to the stationary covariance, which is characterized by its eigenvalues in the Fourier basis. When d goes to ∞ , under appropriate correlation decay assumptions, consistent power-spectrum estimators provide accurate Gaussian stationary models. However, Gaussian models do not take into account coherent structures such as singularities or vortices. Markov Random Fields [24] provide an alternative approach to building low-dimensional models, where conditional probability densities of $X(u)$ given all other $X(u')$ for $u' \neq u$ depend only on values of $X(u')$ over a small neighborhood of u . These models have important applications, but do not scale well to random processes having long range interactions, producing large scale coherent structures.

The Hammersley-Clifford theorem proves that MRFs are particular examples of Gibbs distributions having an exponential density. In his seminal paper, Jaynes [23] interprets statistical physics as an inference of a probability distribution from partial measurements, by maximizing its entropy. In Jaynes words [23], maximizing the entropy of a probability distribution “is maximally noncommittal with regard to missing information.” If $\Phi_d x \in \mathbb{R}^K$ is a K -dimensional vector, which is interpreted as an interaction energy calculated from $x(u)$ for $u \in \Lambda_d$, then the probability distribution μ of maximum entropy, conditioned to $\mathbb{E}_\mu(\Phi_d X) = y$ has a Gibbs exponential density parametrised by Lagrange multipliers. Building a Gibbs model thus amounts to specifying the K -dimensional operator Φ_d . Stationarity is obtained by imposing that $\Phi_d x$ is invariant to translations of x .

This macrocanonical point of view is not appropriate for us because we only know a single realization \bar{x} of X as opposed to the average interaction energy $\mathbb{E}_\mu(\Phi_d X)$. Microcanonical models replace the conditioning on $\mathbb{E}_\mu(\Phi_d X)$ by a conditioning on $\Phi_d \bar{x}$. A microcanonical model is a maximum entropy distribution whose support is limited to points x such that $\Phi_d x$ is nearly equal to $\Phi_d \bar{x}$. Even though we have a single observation, under appropriate ergodicity assumptions, one may be able to approximate the underlying measure μ when d goes to ∞ , by requiring that the microcanonical model converges when d goes to ∞ . The Boltzmann equivalence principle establishes that under appropriate conditions, this microcanonical measure converges to the same Gibbs measure as their macrocanonical counterpart. To guarantee convergence of micro and macrocanonical models to the same stationary Gibbs measure, one considers interaction energies computed as an aver-

age of shift-invariant potentials, having a finite range. Section 2.4 reviews large deviation results proving that if there is no phase transition and if the potential is bounded, then Boltzmann’s equivalence principle is valid when d goes to ∞ .

However, for finite realization sizes $d < \infty$, one may still want to consider microcanonical models not as an approximation of an underlying Gibbs measure, but as genuine density models that can be deployed on real datasets. This is motivated both from a statistical and computational point of view. First, fitting microcanonical models to data avoids the estimation of Lagrange multipliers needed in macrocanonical models. Next, sampling from Gibbs measures is a computationally expensive procedure, relying on MCMC [5] or variational methods [33]. Section 3 studies asymptotic properties of microcanonical measures, and describes a simple sampling algorithm, based on the gradient flow defined by the potential vector. Beginning from a high entropy measure, this algorithm implements a progressive transport converging to the microcanonical set. In particular, we show how the Jacobian of Φ_d dictates both the free energy and the convergence properties of the microcanonical measure; and study conditions under which gradient descent over the microcanonical energy converges to the microcanonical ensemble.

A major issue is to specify a low-dimensional shift-invariant interaction energy Φ_d providing accurate approximations of non-Gaussian phenomena with long range interactions, such as image and audio textures. We construct such models with multiscale sparse representations in Section 4. Long range interactions are taken into account by separating scales with wavelet transforms, which has similarities with renormalization group approaches [4]. Under-determined energy vectors Φ_d result in microcanonical models whose entropy is too large, producing poor density models with limited practical application. Reducing entropy amounts to defining microcanonical sets of small volume. Section 4 explains that this can be achieved by finding wavelets providing sparse representations of realization of X . The resulting energy vector Φ_d is defined from ℓ^1 norms of wavelet coefficients. Coherent structures at each scale are further characterized by a scattering transform [26, 9], which iterates over wavelet transforms and point-wise nonlinearities. The resulting computational architecture has strong similarities with deep convolutional networks.

Finally, we demonstrate the efficiency of multiscale sparse microcanonical models on several synthetic and real-world experiments in Section 5. If the probability density is known, as in the Ising model, then one can evaluate a maximum entropy microcanonical model by verifying that sampling from this model defines typical realizations. When the probability density is unknown, verifying such models remains an open issue. For image and audio textures, one may evaluate qualitatively perceptual differences between the realizations of the original process. Numerical results are evaluated on Ising processes, point processes convolved with patterns, multifractals, image and audio textures.

2 Microcanonical versus Canonical Models

We consider a stationary process $X(u)$ taking its values in an interval $I \subset \mathbb{R}$ for all $u \in \mathbb{Z}^\ell$. We denote by μ the probability measure of this stationary process. Let $\Lambda_d \subset \mathbb{Z}^\ell$ be a cube with d grid points. Microcanonical models described in Section 2.1 are probability densities conditioned by a K -dimensional energy vector $\Phi_d X$ calculated over the restriction of X to Λ_d . We denote by I^{Λ_d} the corresponding product image space. To review its convergence properties when d goes to ∞ , Section 2.2 briefly summarizes the properties of macrocanonical models conditioned by $\mathbb{E}_\mu(\Phi_d X)$. Section 2.4 reviews the convergence properties of micro and macrocanonical models towards Gibbs measures, for shift-invariant interaction energies Φ_d introduced in Section 2.3.

2.1 Microcanonical Models

A microcanonical model is computed from $y = \Phi_d \bar{x}$ for a single realization \bar{x} of X restricted to Λ_d . To estimate the underlying measure μ from a single realization, we need X to satisfy some form of ergodicity, and we shall assume that $\Phi_d X$ concentrates with high probability around $\mathbb{E}_\mu(\Phi_d x)$ when d goes to ∞ :

$$\forall \epsilon > 0, \quad \lim_{d \rightarrow \infty} \text{Prob}_\mu(\|\Phi_d x - \mathbb{E}_\mu(\Phi_d X)\| \leq \epsilon) = 1. \quad (1)$$

If there exists $C > 0$ such that $\|\mathbb{E}_\mu(\Phi_d x)\| \leq C$ then this convergence in probability is implied by a mean-square convergence:

$$\lim_{d \rightarrow \infty} \mathbb{E}_\mu(\|\Phi_d x - \mathbb{E}_\mu(\Phi_d x)\|^2) = 0. \quad (2)$$

The microcanonical set of width ϵ associated to $y = \Phi_d \bar{x}$ is

$$\Omega_{d,\epsilon}^y = \{x \in I^{\Lambda_d} : \|\Phi_d x - y\| \leq \epsilon\}.$$

The concentration property (1) implies that when d goes to ∞ , X belongs to microcanonical sets $\Omega_{d,\epsilon}^y$ of width ϵ_d converging to 0, with a probability converging to 1.

The differential entropy of a probability distribution which admits a density $p(x)$ relatively to the Lebesgue measure is

$$H(p) = - \int p(x) \log p(x) dx. \quad (3)$$

A microcanonical model was defined by Boltzmann as the maximum entropy distribution supported in $\Omega_{d,\epsilon}^y$. If $\Omega_{d,\epsilon}^y$ is compact then it has a uniform density $p_{d,\epsilon}$:

$$p_{d,\epsilon,y}(x) = \frac{1_{\Omega_{d,\epsilon}^y}(x)}{\int_{\Omega_{d,\epsilon}^y} dx}. \quad (4)$$

Its entropy is therefore

$$H(p_{d,\epsilon,y}) = - \int p_{d,\epsilon,y}(x) \log p_{d,\epsilon,y}(x) dx = \log \left(\int_{\Omega_{d,\epsilon}^y} dx \right) . \quad (5)$$

It is the logarithm of the volume of $\Omega_{d,\epsilon}^y$.

The concentration (1) guarantees that the support the measure μ is mostly concentrated in $\Omega_{d,\epsilon}^y$ for large d . The main issue is to construct microcanonical sets which are not too large. The energy Φ_d must thus be adapted in order to build microcanonical sets of minimum volume which satisfy the concentration property (1).

2.2 Macrocanonical Models

Since $\Phi_d X$ concentrates close to $\mathbb{E}_\mu(\Phi_d X)$, one could expect that the maximum entropy distribution conditioned on $\Phi_d X$ converges to the maximum entropy distribution conditioned on $\mathbb{E}_\mu(\Phi_d X)$ when d goes to ∞ . Section 2.3 studies conditions under which this Boltzmann equivalence hypothesis is verified. We begin by reviewing the properties of canonical maximum entropy models conditioned by $\mathbb{E}_\mu(\Phi_d X) = y$.

A canonical distribution has a density which has the same expected energy

$$\mathbb{E}_p(\Phi_d x) = \int \Phi_d x p_d(x) dx = y \quad (6)$$

and which has a maximum entropy

$$H(p) = - \int p(x) \log p(x) dx .$$

The entropy is a concave function of p whereas (6) are linear conditions over p . If $\Phi_d x$ is bounded over I^{Λ_d} then the set of densities p which satisfy the moment conditions (6) is compact. As a consequence, there exists a unique canonical density p_d which maximizes $H(p)$. It is obtained by minimizing the following Lagrangian

$$\mathcal{L}_d(p, \beta) = -H(p) + \langle \beta, \mathbb{E}_p(\Phi_d x) - y \rangle , \quad (7)$$

also called free energy in statistical physics. The Lagrange multipliers $\beta = \{\beta_k\}_{k \leq K}$ are adjusted so that the moment condition (6) is satisfied. The density which minimizes (7) can be written as

$$p_d(x) = \mathcal{Z}^{-1} \exp(-\langle \beta, \Phi_d x \rangle) , \quad (8)$$

where \mathcal{Z} guarantees that $\int p_d(x) dx = 1$ and hence

$$\mathcal{Z} = \int_{I^{\Lambda_d}} \exp(\langle \beta, \Phi_d x \rangle) dx .$$

A direct calculation shows that the resulting maximum entropy is

$$H(p_d) = -\log \mathcal{Z} + \langle \beta, y \rangle . \quad (9)$$

If the probability measure of the restriction of X to Λ_d has a density p relatively to the Lesbegue measure, then we also verify that the Kullback-Liebler divergence

$$KL(p||p_d) = \int_{\Lambda_d} p(x) \log \frac{p_d(x)}{p(x)} dx$$

satisfies

$$KL(p||p_d) = H(p_d) - H(p) \geq 0 .$$

We thus have $p = p_d$ if and only if the maximum entropy is $H(p_d) = H(p)$. Optimizing the interaction energy Φ_d thus amounts to minimizing the resulting maximum entropy $H(p_d)$ [36].

It is not necessary to impose that Φ_d is bounded on I^{Λ_d} . If there exists $\beta \in \mathbb{R}^K$ such that the distribution (8) satisfies the moment condition (6) then it is the unique maximum entropy distribution. However, if $\Phi_d x$ is not bounded then there may not exist such a $\beta \in \mathbb{R}^K$. The vector β can be computed with Metropolis-Hasting type algorithms which sample the Gibbs distribution (8) to estimate $\mathbb{E}_{p_d}(\Phi_d x)$ and iteratively updates β until $\mathbb{E}_{p_d}(\Phi_d x)$ converges to y . However, when d and K are large, this is numerically unfeasible because sampling a high-dimensional probability distribution is computationally very expensive.

2.3 Shift Invariant Finite Range Potentials

Microcanonical densities in (4) and macrocanonical densities in (8) are functions of $\Phi_d x$. These densities remain constant under any transformation of x which leaves $\Phi_d x$ constant. Stationary densities are obtained with translation invariant energies obtained by averaging a shift-invariant potential vector. We review simple examples with \mathbf{l}^1 and \mathbf{l}^2 norms, to illustrate convergence issues of micro and macrocanonical densities when d goes to ∞ .

Shift Invariant Potential For any $x \in I^{\mathbb{Z}^\ell}$ we define a potential $Ux(u) \in \mathbb{R}^K$ for each $u \in \mathbb{Z}^\ell$. We write $T_\tau x(u) = x(u - \tau)$ a translation of x by $\tau \in \mathbb{Z}^\ell$. A potential U is shift-invariant if

$$\forall (x, \tau) \in I^{\mathbb{Z}^\ell} \times \mathbb{Z}^\ell, UT_\tau x = T_\tau Ux .$$

The energy $\Phi_d x$ is computed from the restriction of x in a square $\Lambda_d = [a, b]^\ell$. We extend x over \mathbb{Z}^d into a signal which is $b - a = d^{1/\ell}$ periodic along each of the ℓ generators of the grid \mathbb{Z}^ℓ . With an abuse of notation we write Ux the potential U applied to the periodic extension of x and

$$\Phi_d x = d^{-1} \sum_{u \in \Lambda_d} Ux(u). \quad (10)$$

Observe that $\Phi_d x \in \mathbb{R}^K$ is invariant to periodic translations of x in Λ_d modulo $d^{1/\ell}$.

We say that Ux has a finite range Δ if $Ux(u)$ only depends upon the values of $x(u')$ for $u - u' \in [-\Delta, \Delta]^\ell$. The resulting macrocanonical density (8)

$$p_d(x) = \mathcal{Z}^{-1} \exp(-d^{-1} \sum_{u \in \Lambda_d} \langle \beta, Ux(u) \rangle) \quad (11)$$

is a Markov random field over cliques $[u - \Delta, u + \Delta]^\ell$ around each u . In the following we shall impose such a condition but Δ may be very large. In turbulence flows, Δ is the integral scale beyond which structures become uncorrelated. Before reviewing the general convergence properties of the resulting micro and macrocanonical densities we consider two important examples obtained with \mathbf{l}^r norms.

Convergence of \mathbf{l}^r macro and microcanonical densities The potential $Ux(u) = |x(u)|^r$ for $u \in \mathbb{Z}$ defines an \mathbf{l}^r norm energy over intervals $\Lambda_d = [1, d] \subset \mathbb{Z}$.

$$\Phi_d x = d^{-1} \|x\|_r^r = d^{-1} \sum_{u \in \Lambda_d} |x(u)|^r. \quad (12)$$

The macrocanonical density p_d defined by $\mathbb{E}_{p_d}(\Phi_d x) = y \geq 0$ is $p_d(x) = \mathcal{Z}^{-1} e^{-\beta d^{-1} \|x\|_r^r}$ for some $\beta > 0$. It is the density of a vector X_d of d i.i.d random variables having an exponential distribution $\alpha e^{-\beta|z|^r}$.

A microcanonical density $p_{d,\epsilon}$ is uniform over $\Omega_{d,\epsilon}^y = \{x \in \mathbb{R}^d : |d^{-1} \|x\|_r^r - y| \leq \epsilon\}$, which is a thin shell around an \mathbf{l}^r ball in \mathbb{R}^d . It is the density of a random vector $X_{d,\epsilon}(u)$ for $u \in \Lambda_d$. For a fixed $m > 0$, when d goes to ∞ and ϵ goes to zero then the joint density of $X_{d,\epsilon}(1), \dots, X_{d,\epsilon}(m)$ converges with a total variation distance to i.i.d random variables having an exponential distribution $\alpha e^{-\beta|z|^r}$ [3], and $\mathbb{E}(|X_{d,\epsilon}(u)|^r)$ converges to y . The microcanonical distribution thus converges to the macrocanonical distribution. This family of results has a long history, first proved in 1906 by Borel [6] for $r = 2$ and in 1987 by Diaconis and Freeman for $r = 1$ [16].

Intersections of \mathbf{l}^1 and \mathbf{l}^2 balls The situation becomes already more complex for the two-dimensional potential $Ux(u) = (|x(u)|^1, |x(u)|^2)$ which defines an energy $\Phi_d x = (d^{-1} \|x\|_1, d^{-1} \|x\|_2^2)$ over intervals $\Lambda_d = [1, d] \subset \mathbb{Z}$.

Micro and macrocanonical densities are not defined over the same range of moment values. One can verify that there exists a unique maximum entropy density p_d conditioned by $\mathbb{E}_{p_d}(\Phi_d x) = y$ if and only if

$$d^{-1} < \frac{y_2}{y_1^2} \leq 2,$$

in which case

$$p_d(x) = \mathcal{Z}^{-1} e^{-d^{-1} (\beta_1 \|x\|_1 + \beta_2 \|x\|_2^2)}.$$

The microcanonical set $\Omega_{d,\epsilon}^y = \{x : \|\Phi_d x - y\| \leq \epsilon\}$ is thin shell around the intersection of the simplex $\|x\|_1 = d y_1$ and the sphere $\|x\|_2^2 = d y_2$. Since $\|x\|_2^2 \leq \|x\|_1^2 \leq d\|x\|_2^2$, this intersection is non-empty over a wider range defined by

$$d^{-1} \leq y_2/y_1^2 \leq d.$$

When $d^{-1} < \frac{y_2}{y_1^2} \leq 2$, micro and macrocanonical densities have the same limit when d goes to ∞ and ϵ goes to zero. For m fixed, S. Chatterjee [12] proves that the joint microcanonical density of $X_{d,\epsilon}(1), \dots, X_{d,\epsilon}(m)$ converges to i.i.d random variables having an exponential distribution equal to $\alpha e^{-\beta_1|z| - \beta_2|z|^2}$, and $(\mathbb{E}(|X_{d,\epsilon}(u)|), \mathbb{E}(|X_{d,\epsilon}(u)|^2))$ converges to y . If $y_2/y_1^2 = 2$ then $\beta_2 = 0$.

When $y_2/y_1^2 > 2$ the macrocanonical density is not defined. The microcanonical set contains very sparse signals which are not captured by exponential distributions. In this case, Chatterjee [12] proves that when d goes to ∞ and ϵ to 0, $X_{d,\epsilon}$ has one large coefficient randomly located at some $u_0 \in \Lambda_d$ for which $X_{d,\epsilon}^2(u_0) \sim d(y_2 - 2y_1^2)$ with a probability which tends to 1. All other coefficients have a much smaller $O(y_1)$ amplitude. For m fixed, $X_{d,\epsilon}(1), \dots, X_{d,\epsilon}(m)$ converge in law to i.i.d random variables having marginals equal to $e^{-\beta_1|z|}$, but there is no convergence of moments. In this range, the Boltzmann equivalence principle is violated since macrocanonical densities are not defined.

2.4 Convergence to Gibbs Measures

Micro and macrocanonical densities are defined over configurations x specified in a finite cube Λ_d of dimension ℓ . Let $\Phi_d x$ be an energy vector computed by averaging a shift-invariant, finite range potential Ux . To compute estimators which converge when d goes to ∞ , we need to ensure that microcanonical densities converge in the moments sense. We consider the limit among measures defined on the configuration space $I^{\mathbb{Z}^\ell}$, with the product topology of Borel fields on the interval $I \subset \mathbb{R}$. It thus amounts to verifying the Boltzmann equivalence principle between micro and macrocanonical models, and their convergence to Gibbs measures introduced by Landford [18]. The previous example shows that difficulties arise if x is not bounded. When I is a bounded interval, we review convergence results of micro and macrocanonical densities towards stationary Gibbs measures.

Convergence of Canonical models In the bounded case, macrocanonical distributions are unique minimizers of the Lagrangian (7). When d goes to ∞ , the limit Gibbs measure is defined by normalizing this Lagrangian so that it converges to a variational problem defined over a stationary measure μ . Suppose that μ exists. Since Ux is shift-invariant, $\mathbb{E}_\mu(Ux(u)) = \mathbb{E}_\mu(Ux)$ does not depend upon the grid point u . Suppose that μ has no long range correlation so that boundary values have a negligible influence. Since $\Phi_d x$ is an average of $Ux(u)$ in Λ_d it follows that

$$\lim_{d \rightarrow \infty} \mathbb{E}_\mu(\Phi_d x) = \mathbb{E}_\mu(Ux) .$$

The entropy rate $F(\mu)$ is defined by considering the restriction μ_d of μ on the finite dimensional configuration space I^{Λ_d} . Let q_d be the density of μ_d relatively to the Lebesgue measure. If μ has a finite range correlation we expect that $H(q_d)$ grows linearly with d . The entropy rate is defined by

$$F(\mu) = \lim_{d \rightarrow \infty} d^{-1} H(q_d) . \quad (13)$$

Normalizing the free energy Lagrangian (7) by d and taking the limit when d goes to ∞ defines a new Lagrangian

$$\mathcal{L}_\infty(\mu, \beta) = -F(\mu) + \langle \beta, \mathbb{E}_\mu(Ux) - y \rangle . \quad (14)$$

Gibbs measures minimize this Lagrangian over the space of stationary measures for β fixed.

If U is a bounded, finite range and continuous potential, then one can prove [15, 21] that the set of Gibbs measures which minimize this Lagrangian is a non-empty, convex and compact set of measures. In general the solution is not unique because contrarily to the finite Lagrangian (7) where $-H(p_q)$ is strictly convex, the entropy rate $F(\mu)$ is affine [15, 21]. This implies that depending upon boundary conditions in Λ_d macrocanonical densities may converge to different Gibbs measures, which is a phase transition phenomena.

Periodic boundary conditions over the finite cube Λ_d simplify computational algorithms, but they are artificial. The limit Gibbs measure will not depend upon these boundary conditions if it is unique, and hence if there is no phase transition. This happens when there is no long range interactions, so that boundary values do not condition the probability distributions of far away values. In this paper, we concentrate on problems where there is no such phase transition.

Microcanonical convergence The Boltzmann equivalence principle assumes that micro and macrocanonical measures converge to the same Gibbs measure. This property is verified by showing that it is also solution of the variational problem (14). The condition $\mathbb{E}_\mu(\Phi_d x) = y$ is now replaced by $\|\Phi_d x - y\| \leq \epsilon$.

Since Φ_d is an average of translated potential vectors

$$\Phi_d x = d^{-1} \sum_{u \in \Lambda_d} U T_u x ,$$

it can be expressed in terms of the empirical measure $R_d x = d^{-1} \sum_{u \in \Lambda_d} \delta_{T_u x}$ by

$$\Phi_d x = \int U x R_d x dx = \mathbb{E}_{R_d x}(U x) \quad (15)$$

Since $\Phi_d x = \mathbb{E}_{R_d}(U x)$, microcanonical densities are conditioned by $\|\mathbb{E}_{R_d x}(U x) - y\| \leq \epsilon$. The link with entropy rate is provided by proving a large deviation property [14]. It

guarantees that for a normalized Lebesgue measure, the log probability that R_dx belongs to a set of measures A converges to the maximum entropy rate of measures in A , that we shall write:

$$\text{Prob}(R_dx \in A) \sim e^{-d \sup_{\nu \in A} F(\nu)} . \quad (16)$$

It follows that R_dx conditioned by $\|\mathbb{E}_{R_dx}(Ux) - y\| \leq \epsilon$ concentrates with high probability in sets of measures having a nearly maximum entropy rate.

If U is continuous, bounded, with a finite range then one can prove [15, 21] that when d goes to ∞ and ϵ goes to zero then microcanonical distributions converge for an appropriate topology, to a limit measure which minimizes the same Lagrangian (14) as the one obtained from canonical densities. If there is no phase transition, so that the canonical measure converges to a unique Gibbs measure μ , then this limit is the same for canonical and microcanonical measures. More specifically, if $f(x)$ is a bounded and continuous function defined for any $x \in I^{\mathbb{Z}^\ell}$, then the expected value of f computed over Λ_d with microcanonical and macrocanonical measures converge to $\mathbb{E}_\mu(f(x))$ when d goes to ∞ . We thus have a convergence for all bounded moments.

Gaussian processes Convergence to Gibbs measures does not necessarily require that the values of x remain bounded. Gaussian stationary measures are important examples of Gibbs measures where x takes its values in $I = \mathbb{R}$. They are obtained with a quadratic potential $Ux = \{U_k x\}_{k \leq K}$ which is shift-invariant over the grid \mathbb{Z}^d . Suppose that

$$U_k x(u) = |x \star h_k(u)|^2 = \left| \sum_{m \in \mathbb{Z}^d} x(u-m) h_k(m) \right|^2 ,$$

where each h_k has a support in $[-\Delta, \Delta]$.

If $x \in \mathbb{R}^{\Lambda_d}$ then Ux is computed by extending x on \mathbb{Z}^ℓ with a periodic extension beyond boundaries. This is equivalent to compute convolutions with periodic filters

$$h_{d,k}(n) = \sum_{m \in \mathbb{Z}^\ell} h_k(n - md^{1/\ell}) \quad (17)$$

and a circular convolution

$$U_k x(u) = |x \star h_{d,k}(u)|^2 = \left| \sum_{m \in \Lambda_d} x(m) h_{d,k}(n-m) \right|^2 . \quad (18)$$

The energy $\Phi_d x$ is thus a vector of normalized \mathbf{I}^2 norms:

$$\Phi_d x = \left\{ d^{-1} \sum_{u \in \Lambda_d} |x \star h_{d,k}(u)|^2 = d^{-1} \|x \star h_{d,k}\|_2^2 \right\}_{k \leq K} . \quad (19)$$

If all $\hat{h}_k(\omega)$ do not vanish then Varadham and Donsker [17] prove that when d goes to ∞ microcanonical and macrocanonical random vectors converge to a Gaussian stationary process μ whose power-spectrum is

$$P_\mu(\omega) = \left(\sum_{k=1}^K \beta_k |\hat{h}_k(\omega)|^2 \right)^{-1}. \quad (20)$$

3 Sampling Microcanonical Models

Sampling microcanonical measures is a classic problem in statistical mechanics, typically approached by adapting MCMC algorithms to ensure that the chain remains in the microcanonical ensemble, such as Creutz's algorithm [13]. Whereas these algorithms have theoretical guarantees, their numerical effectiveness on high-dimensional problems is hindered by the slow mixing speed of the Markov Chain [13]. This motivated the use of approximated sampling algorithms, based on gradient descent, as illustrated by the early texture synthesis of [22, 30] and more recently [19]. The goal of this section is to study the gradient-descent microcanonical sampling and its convergence properties to the microcanonical measure.

3.1 Entropy and Jacobian

The first step to relate gradient descent sampling to the microcanonical measure is to reveal how the entropy rate depends upon the Jacobian of the energy vector. The main result of this section proves that under appropriate conditions, the microcanonical free energy converges, without relying on the underlying macrocanonical model.

We consider the shift-invariant potentials from Section (2.3), and the corresponding microcanonical distributions, defined as uniform density on compact sets of the form

$$\Omega_{d,\epsilon}^y = \{x : \|\Phi_d x - y\| \leq \epsilon\}.$$

We saw in (5) that the entropy is

$$H(p_{d,\epsilon}^y) = - \int p_{d,\epsilon}^y(x) \log p_{d,\epsilon}^y(x) dx = \log \left(\int 1_{\Omega_{d,\epsilon}^y}(x) dx \right). \quad (21)$$

Thanks to the construction of Φ_d as a spatial average of localized, translation covariant potentials, the i -th column $J_i \Phi_d(x) = \left(\frac{\partial \Phi_{d,k}}{\partial(x_i)}(x) \right)_{k \leq K} \in \mathbb{R}^K$ only depends upon the restriction of x in the $(i \pm 2\Delta)^\ell$ coordinates. Moreover, thanks to the covariant structure of U , one can verify that

$$\forall i \leq d, \quad J_i \Phi_d(x) = J_1 \Phi_d(T_{-i}x) = d^{-\ell} \sum_{|l| \leq \Delta} \partial_{x_1} U(T_{-i}x)(l),$$

so the global properties of the Jacobian $J\Phi_d(x)$ can be derived from the Jacobian of the potential

$$\begin{aligned} \bar{J}U : \mathbb{R}^{2\Delta+1} &\rightarrow \mathbb{R}^K \\ \bar{x} &\mapsto \sum_{|l|\leq\Delta} \partial_{x_1} U(\bar{x})(l) . \end{aligned} \quad (22)$$

We shall make the following assumptions on U :

- (A) U is Lipschitz on compact sets, which implies that for any compact $C \subset E^{\Lambda_d}$ there exists $\beta \geq 0$ such that

$$\forall (x, x') \in C^{2d} \quad , \quad \|\Phi_d x - \Phi_d(x')\|_2 \leq \beta \|x - x'\|_2 . \quad (23)$$

It also implies that $|J\Phi_d(x)| \leq \beta^K$ for $x \in C$. We denote $\beta = \text{Lip}_\Phi$.

- (B) We shall also suppose that Φ_d^{-1} maps compact sets C to compact sets, which means that

$$\Phi_d^{-1}(C) = \{x \in \Omega_d : \Phi_d(x) \in C\} \text{ is compact.} \quad (24)$$

It results that $\Phi_d^{-1}(y)$ is a compact and Lipschitz manifold whose dimension is typically $d - K$, besides degenerated cases. For example, if Φ_d includes a norm $\|x\|_p$, this condition is satisfied.

Lastly, we need to control the integrability of $|J\Phi_d|^{-1}$: For each y and any sufficiently small $\epsilon > 0$, $|J\Phi_d(x)|^{-1}$ is integrable in $\Omega_{d,\epsilon}^y$. The following gives a sufficient condition which depends only on the potential function.

- (C) For some $R > 0$, let \bar{X} be drawn from the uniform measure in the ball $B(2\Delta + 1, R)$ and $Z = \bar{J}U(\bar{X}) \in \mathbb{R}^K$ be the random vector obtained by applying the mapping $\bar{J}U$ defined in (22). We shall suppose that there exists $\eta > 0$ such that

$$\forall S \subset \mathbb{R}^K \text{ Lebesgue measurable} , \quad P(Z \in S) \lesssim |S|^\eta . \quad (25)$$

This condition assumes that the differential of U does not concentrate too much on a low-dimensional subspace of \mathbb{R}^K , nor in a discrete subset, but it does not require that its distribution is absolutely continuous with respect to the Lebesgue measure. We shall see next that potentials of the form $Ux = \{|x \star h_k|^p\}_{k \leq K}$ with $p = 1, 2$ with complex filters h_k define an integrable $|J\Phi_d|^{-1}$.

We denote by ∂A the frontier of a set A and by $A^\circ = A - \partial A$ the interior of A , and by \bar{A} the complement of A . We also denote by $|J\Phi_d(x)| = \sqrt{\det(J\Phi_d(x)J\Phi_d(x)^T)}$ the K -dimensional determinant of $J\Phi_d$, and by $d\mathcal{H}(x)^L$ the L -dimensional Hausdorff measure. The following theorem computes the entropy of a microcanonical process from a change of variable metric, which depends upon the Jacobian of the interaction energy Φ_d . The theorem derives a microcanonical free energy which converges when d goes to ∞ .

Theorem 3.1. *Suppose U verifies (A), (B) and (C) above. Then the following properties are verified:*

(i)

$$H(p_{d,\epsilon}^y) = \log \int_{\|z-y\| \leq \epsilon} \gamma_d(z) dz , \quad (26)$$

where γ_d is the change of variable metric which satisfies

$$\gamma_d(y) = \int_{\Phi_d^{-1}(y)} |J\Phi_d(x)|^{-1} d\mathcal{H}^{d-K}(x) < \infty \quad \text{a.e.} \quad (27)$$

and has a finite integral on compact sets.

(ii) *The function γ_d is strictly positive in the interior of $\Phi_d(\Omega_d)$, up to a thin shell on the border; ie, on sets $C_d \subset \Phi_d(\Omega_d)$ satisfying*

$$\sup_{y \in C_d} \text{dist}(y, \overline{\Phi_d(\Omega_d)}) \leq c/d ,$$

for some constant c .

(iii) *Suppose that either $\Delta = 1$, or that Ux is a bounded potential. Then, for each $\epsilon > 0$, the entropy rate $d^{-1}H(p_{d,\epsilon}^y)$ converges as $d \rightarrow \infty$ and satisfies*

$$-\infty < \lim_{d \rightarrow \infty} d^{-1}H(p_{d,\epsilon}^y) \leq C\|y\|^2 , \quad (28)$$

where C is a universal constant.

The proof is in Appendix A. This theorem thus provides a notion of free energy of a microcanonical ensemble for general Φ_d in the thermodynamical limit $d \rightarrow \infty$, without resorting to the canonical equivalence. An important remark is to compare the conditions of Theorem 3.1 with those that ensure the convergence of the microcanonical and macrocanonical measures. In [32, 14] this equivalence is established for bounded, finite-range potentials U , which we also require to prove part (iii). Our result highlights the close connection between free energy and the Jacobian properties of the energy, determined by $\gamma_d(y)$ via the coarea formula, although the validity of the convergence in more general conditions remains an open question.

This paper studies interaction energies Φ_d based on \mathbf{l}^2 and \mathbf{l}^1 norms. The next proposition proves that such interaction energies satisfy the assumptions of Theorem 3.1. The proof is in Appendix B.

Proposition 3.2. *Φ_d satisfies assumptions (A), (B) and (C) in the following cases:*

(i) $\Phi_d(x) = \{d^{-1}\|x \star h_k\|_2^2\}$ with h_k linearly independent.

(ii) $\Phi_d(x) = \{d^{-1}\|x\|^2, d^{-1}\|x\|_1\}$.

(iii) $\Phi_d(x) = \{d^{-1}\|x\|^2, d^{-1}\|x \star h_k\|_1\}$ with h_k linearly independent such that $|\hat{h}_k(-\omega)| \neq |\hat{h}_k(\omega)|$ for all ω .

3.2 Microcanonical Gradient Descent

This section describes a gradient descent algorithm which computes an approximate sampling of microcanonical processes, with a Gaussian white noise initialization. Its convergence to the microcanonical ensemble is established for appropriate choices of the potential function, and we also give a bound on the entropy rate of the resulting random vector.

Despite having intractable partition functions, sampling from canonical models is possible thanks to Markov-Chain Monte-Carlo methods, which construct stochastic markov chains whose stationary limit is the canonical model in question. We consider here the alternative framework corresponding to the microcanonical model, in which a Markov chain is replaced by a gradient flow determined by the microcanonical energy function, which under appropriate conditions is also guaranteed to converge to the correct model. Approximate microcanonical sampling using gradient descent has been successfully used on high-dimensional sampling problems such as texture synthesis; see [22, 30], and is conceptually closely related to Hamiltonian Monte-Carlo [5], in which the gradient information of the Hamiltonian is used to efficiently explore the typical set. Another closely related sampling algorithm that avoids the estimation of canonical parameters is the so-called herding algorithm by Welling [35], which produces ‘pseudo-samples’ of a microcanonical model in a deterministic fashion by solving a sequence of primal-dual updates.

We embed all processes, including binary processes such as Ising and Bernoulli over an interval $I = [a, b]$ of \mathbb{R} . Let Φ_d be a shift-invariant function as defined in Section 2.3 and $y \in \Phi_d(I^{\Lambda_d})$. We suppose here that Φ_d satisfies assumptions (A), (B), (C).

The algorithm will iteratively transport an initial high-entropy measure μ_0 towards measures whose support converges towards $\Phi_d^{-1}(y)$. The measure transportation is performed by considering the scalar energy

$$\mathcal{E}_y(x) = \frac{1}{2} \|\Phi_d(x) - y\|^2 \quad (29)$$

and diffeomorphisms of the form

$$\varphi_n(x) = x - \kappa_n \nabla \mathcal{E}_y(x) = x - \kappa_n J\Phi_d(x)^T (\Phi_d(x) - y) , \quad (30)$$

with $\kappa_k < \frac{1}{\beta}$, where β is the Lipschitz constant of $\bar{J}U$. These diffeomorphisms define the update

$$\mu_{n+1} := \varphi_{n,\#} \mu_n \quad (31)$$

using the standard pushforward measure $f_{\#}(\mu)[A] = \mu[f^{-1}(A)]$ for A μ -measurable.

Samples from μ_n are thus obtained by transforming samples x_0 from μ_0 with the diffeomorphism $\bar{\varphi} = \varphi_n \circ \varphi_{n-1} \cdots \circ \varphi_1$, which corresponds to n steps of gradient descent initialized with x_0 :

$$x_{l+1} = x_l - \kappa_l J\Phi_d(x_l)^T (\Phi_d(x_l) - y) .$$

We choose μ_0 to be the maximum entropy measure of I^{Λ_d} if I is bounded, and the Gaussian measure with known energy σ^2 otherwise. When I is a bounded interval, we consider a

diffeomorphism g that maps \mathbb{R}^d into I , and consider the change of variables $y = g^{-1}(x)$, $x \in \mathbb{R}^{\Lambda_d}$ and we redefine Φ_d by $\Phi_d \circ g$ so that it is now defined over \mathbb{R}^{Λ_d} . In all our experiments, we construct g as a sigmoid along each coordinate: $g(x) = (\sigma(x_1), \dots, \sigma(x_{\Lambda_d}))$, with $\sigma(t) = (1 + \exp(-t/c))^{-1}$ with a small value of c .

3.3 Convergence of Microcanonical Gradient Descent

The main result of this section characterizes the limit measure μ_∞ obtained by the gradient descent iterative scheme (31). We shall use the characterization of stable solutions from [25, 29] based on the second-order analysis of critical points of (29). Such analysis reveals that gradient descent methods do not get stuck at critical points which are *strict saddles* — in which at least one Hessian eigenvalue is strictly negative, since the set of initialization parameters corresponding to the non-negative spectrum has measure 0 relative to μ_0 .

Definition 3.3. *We say that $\Phi_d = (\phi_1, \dots, \phi_K)$ has the strict saddle condition if Φ_d is at least \mathbf{C}^2 and for each $v \in \text{Null}(J\Phi_d(x)^\top) \subseteq \mathbb{R}^K$, $v \neq 0$, the matrix*

$$\sum_{k \leq K} v_k \nabla^2 \phi_k(x) + J\Phi_d(x)^\top J\Phi_d(x) \quad (32)$$

has at least one strictly negative eigenvalue, where $\nabla^2 \phi_k$ is the Hessian of ϕ_k .

The following theorem, proved in Appendix C, establishes basic properties of the distribution generated by gradient descent, including sufficient conditions for its convergence to the microcanonical ensemble.

Theorem 3.4. *Assume Φ_d is \mathbf{C}^2 and satisfies property (B) (24). Suppose that Φ_d is Lipschitz with $\text{Lip}_{\Phi_d} = \beta$ and that $\nabla \Phi_d$ is also Lipschitz, with $\text{Lip}_{\nabla \Phi_d} = \eta$. Let $y \in \Phi_d(I^{\Lambda_d})^\circ$. Then:*

- (i) μ_n is stationary for each n .
- (ii) *If Φ_d satisfies the strict saddle condition, then (29) has no poor local minima. Moreover, if $|J\Phi_d(x)| > 0$ for all $x \in \Phi_d^{-1}(y)$, then μ_n converges almost surely to μ_∞ , which is supported in the microcanonical ensemble $\Phi_d^{-1}(y)$ with appropriate choice of learning rate κ_n ; that is, $A \notin \Phi_d^{-1}(y) \Rightarrow \mu_\infty(A) = 0$.*
- (iii) *The entropy rate $d^{-1}H(\mu_n)$ satisfies*

$$d^{-1}H(\mu_n) \geq d^{-1}H(\mu_0) - \left(1 - \frac{K}{d}\right) \eta \sum_{n' \leq n} \kappa_{n'} r_{n'} - \frac{K}{d} \beta^2 \sum_{n' \leq n} \kappa_{n'}, \quad (33)$$

where $r_n = \mathbb{E}_{\mu_n} \sqrt{\mathcal{E}_y(x)}$ is the average distance to the microcanonical ensemble at iteration n .

This theorem thus gives sufficient conditions for the gradient descent sampling to converge towards the microcanonical ensemble (part *ii*), and bounds how it approximates the maximum entropy microcanonical measure (part *iii*).

Let us now qualitatively relate our entropy rate lower bound (33) with the maximum entropy rate. We saw in Theorem 3.4 that the entropy rate of the microcanonical measure can be measured with the co-area formula as $d^{-1}H(p_{d,\epsilon}^y) = d^{-1} \log \int_{\|z-y\| \leq \epsilon} \gamma_d(z) dz$ and that $\gamma_d(z) > 0$ in the interior of $\Phi_d(I^{\Lambda_d})$. As $\epsilon \rightarrow 0$, we can interpret the previous formula in terms of an $L^1(\mathbb{R}^K)$ approximate identity $h_\epsilon(z) = C_K \epsilon^{-K} \mathbf{1}_{\|z\| \leq \epsilon}(z)$:

$$C_K \epsilon^{-K} \int_{\|z-y\| \leq \epsilon} \gamma_d(z) dz = \gamma_d \star h_\epsilon(y) \rightarrow \gamma_d(y) \quad \text{as } \epsilon \rightarrow 0$$

in $L^1(\mathbb{R}^K)$. One can verify that, by possibly reparametrising ϵ , this implies pointwise convergence for almost every y , so

$$\left| \log \left(C_K \epsilon^{-K} \gamma_{d,\epsilon}^y \right) - \log \gamma_d(y) \right| \xrightarrow{\epsilon \rightarrow 0} 0, \quad a.e., \quad (34)$$

which shows that the entropy rate $d^{-1} \log \gamma_{d,\epsilon}^y$ of the ϵ -thick microcanonical model diverges as $\frac{K}{d} \log \epsilon$ as $\epsilon \rightarrow 0$, in accordance with the fact that the microcanonical measure does not admit a density relative to the d -dimensional Lebesgue measure.

This divergence of the entropy rate as $\epsilon \rightarrow 0$ is also present in the lower bound (33); let us now argue how the two singularities can be “aligned” under appropriate assumptions. Indeed, for gradient descent to converge we require that $\sum_n \kappa_n = \infty$, so the second term in (33) diverges. If we assume that there exists a choice of learning rate κ_n , such that the gradient descent converges to its global optima, and its rate satisfies

$$r_n \simeq e^{-\beta^2 \sum_{n' \leq n} \kappa_{n'}}, \quad (35)$$

we can then identify the equivalent ϵ_n after n iterations from (33) as $\epsilon_n \simeq e^{-\beta^2 \sum_{n' \leq n} \kappa_{n'}}$, since by definition the energy r_n measures the average distance to the microcanonical ensemble, thus $r_n \simeq \epsilon_n$. For instance, assuming $\kappa_n \sim n^{-1}$, we obtain

$$r_n \simeq \epsilon_n \simeq e^{-\beta^2 \sum_{n' \leq n} (n')^{-1}} \simeq e^{-\beta^2 \log n} \simeq n^{-\beta^2}.$$

It follows that for d sufficiently large and an initial measure μ_0 such that $\kappa_n r_n \approx C n^{-1-\beta^2}$ for $n \geq 0$, after removing the singular part we have

$$d^{-1}H(\mu_\infty) \geq d^{-1}H(\mu_0) - \left(1 - \frac{K}{d}\right) \eta \sum_{n'=1}^{\infty} \kappa_{n'} r_{n'} \approx d^{-1}H(\mu_0) - C \eta \beta^{-2},$$

which provides a positive entropy rate lower bound as soon as $C \eta \beta^{-2} < d^{-1}H(\mu_0)$.

The sufficient condition for μ_n to converge to a limit measure μ_∞ requires $|J\Phi_d(x)| > 0$ for $x \in \Phi_d^{-1}(y)$, which for certain choices of Φ may be hard to check. The following corollary, proved in Section D, provides an alternative sufficient condition which is stronger — but easier to evaluate.

Corollary 3.5. *If Φ_d is C^∞ and Lipschitz and satisfies the strict saddle condition, then μ_n converges for any $y \in \Phi_d(I^{\Lambda_d})$ up to a set of zero measure, and μ_∞ is supported in the microcanonical ensemble.*

Now we investigate which energy functions Φ_d satisfy the assumptions of previous theorem. The next theorem proves that the \mathbf{l}^2 ellipsoid representation satisfies the strict saddle condition, and therefore the microcanonical gradient descent has no poor local minima.

Theorem 3.6. *If $\Phi_d(x) = \{d^{-1}\|x \star h_k\|_2^2\}_k$ with linearly independent h_k , then Φ_d satisfies the strict saddle condition and $|J\Phi_d(x)| > 0$ for $x \in \Phi_d^{-1}(y)$ with $y \in \Phi_d(I^{\Lambda_d})^\circ$, and therefore μ_∞ is supported in the microcanonical ensemble.*

A current limitation of the convergence analysis is that it relies on smoothness properties of Φ_d , thus leaving out of scope the \mathbf{l}^1 -based representations. This limitation is intrinsic to the convergence analysis of non-smooth, non-convex optimization methods, which provides no guarantees using simple gradient descent. The analysis of other algorithms such as ADMM [34] or gradient sampling [11] in such conditions is left for future work. Another limitation of Theorem 3.6 is that it does not cover the setting where I is a bounded interval — this extension is also left for future work.

In general, the assumptions that ensure the convergence of the gradient descent microcanonical sampling won't be satisfied. For instance, the convergence analysis in presence of non-smooth coordinates remains an open question, despite good empirical performance. In this context, the performance of the microcanonical sampling model can be improved by adding new energy components into Φ_d , in such a way that the resulting gradient descent algorithm enjoys better convergence. Next section shows that a particularly effective mechanism is to consider multiscale energy components, even in models whose Gibbs distribution is determined at a single scale, such as Ising. This is closely related to the Renormalization Group approaches to study Markov Random Fields.

4 Wavelet Scattering Models

We study classes of Gibbs measures obtained with potential vectors computed with wavelet transforms in order to separate variability at different scales. The use of wavelet transforms is motivated by different point of views. In statistical physics, it is grounded in renormalization group approaches, but it is also motivated from a probabilistic and harmonic analysis point of view, to approximate multiscale phenomena.

4.1 Wavelet Transform ℓ^2 Norms

Random processes having a long correlation length involve interactions at long distances and hence a potentially large number of interacting variables. Renormalization group calculations and multiscale approaches are approximating these interactions by aggregating local interactions, which appear at different scales. This scale separation is performed by a wavelet transform, which computes signal variations at different scales through convolutions with dilated wavelets. Relations with renormalization groups are studied in [4].

Most physical, image or audio processes are stable to small deformations. A small deformation of a typical realization of X remains a typical realization of X . This prior information requires to define microcanonical models which are also stable to deformations. This property is also achieved by separating scales with wavelets.

Wavelet Transform Let us first review the main properties of wavelet transforms. We define Q mother wavelets $\psi_q(u)$ for $u \in \mathbb{R}^\ell$. They have a zero average $\int \psi_q(u) du = 0$ and a support in $[-C, C]^\ell$. Each of these wavelet is dilated by a 2^j factor

$$\psi_{j,q}(u) = 2^{-\ell j} \psi_q(2^{-j}u). \quad (36)$$

Wavelet coefficients are defined by convolutions $x \star \psi_{j,q}(u)$. If x is defined on a cube $\Lambda_d \subset \mathbb{Z}^\ell$, then u is discretized on this square grid. Convolutions are defined by extending x into a periodic signal over \mathbb{Z}^ℓ . We showed in (18) that it is equivalent to compute circular convolutions with periodic wavelet filters (43). Discrete periodic wavelets $\psi_{j,q}(u)$ are band-pass filters with a zero average $\sum_{u \in \Lambda_d} \psi_{j,q}(u) = 0$.

Wavelet coefficients $x \star \psi_{j,q}(u)$ capture the high frequencies of x for $1 \leq j \leq J$. The support of $\psi_{j,q}$ is included in $[-C2^j, C2^j]^\ell$, and the minimum scale is limited by the sampling interval, whereas the maximum scale 2^J is limited by the width $d^{1/\ell}$ of Λ_d . For d large, it is fixed by the maximum correlation scale of the random process which is analyzed. The remaining low frequencies are carried by a low-pass filter $\phi_J(u) = 2^{-Jd} \phi(2^{-J}u)$, whose support is also included in $[-C2^J, C2^J]$. The resulting wavelet transform is

$$Wx = \left\{ x \star \phi_J, x \star \psi_{j,q} \right\}_{j \leq J, q \leq Q}. \quad (37)$$

It separates the lowest frequencies $x \star \phi_J$ from the variations at all other scales carried by each $x \star \psi_{j,q}$.

The wavelet transform operator W is bounded and has a bounded inverse if the wavelets have Fourier transforms which cover the whole frequency domain. Let $\hat{x}(\omega)$ denote the discrete Fourier transform of $x(u)$ for $u \in \Lambda_d$. If there exists $\gamma < 1$ such that

$$\forall \omega, \quad 1 - \gamma \leq |\hat{\phi}_J(\omega)|^2 + \frac{1}{2} \sum_{j,q} (|\hat{\psi}_{j,q}(\omega)|^2 + |\hat{\psi}_{j,q}(-\omega)|^2) \leq 1 \quad (38)$$

then for any $x \in I^{\Lambda_d}$

$$(1 - \gamma)\|x\|_2^2 \leq \|x \star \phi_J\|_2^2 + \sum_{j,q} \|x \star \psi_{j,q}\|_2^2 \leq \|x\|_2^2. \quad (39)$$

It is proved by multiplying (38) with $|\hat{x}(\omega)|^2$ and applying the Plancherel equality. This property implies that W is a contractive and invertible operator, and its inverse has a norm smaller than $(1 - \gamma)^{-1/2}$. If $\gamma = 1$ then W is an isometry.

Let us define a quadratic potential

$$Ux = \{|x \star \phi_J|^2, |x \star \psi_{j,q}|^2\}_{j \leq J, q \leq Q}. \quad (40)$$

Since all filter support are included in $[-C2^J, C2^J]$, it has a finite range $\Delta = C2^J$. When x is defined over a cube Λ_d then Ux is computed by periodizing x which is equivalent to periodizing the wavelet filters and replacing convolutions with circular convolutions, as shown in (18). To simplify notations we shall still write ϕ_J and $\psi_{j,q}$ the periodized filters. According to (19) the energy over a cube Λ_d is given by normalized \mathbf{I}^2 norms

$$\Phi_d x = \{d^{-1}\|x \star \phi_J\|_2^2, d^{-1}\|x \star \psi_{j,q}\|_2^2\}_{j \leq J, q \leq Q}. \quad (41)$$

We saw in (20) that the resulting canonical and microcanonical processes converge to a stationary Gaussian process whose power spectrum is

$$P_\mu(\omega) = \left(\beta_J |\hat{\phi}_J(\omega)|^2 + \sum_{j \leq J, q \leq Q} \beta_{j,q} |\hat{\psi}_{j,q}(\omega)|^2 \right)^{-1}. \quad (42)$$

4.2 Scattering Transform for Sparsity

Many non-Gaussian random processes have realizations which have a sparse wavelet representation, due to isolated sharp transitions. To capture this sparsity, \mathbf{I}^2 norms are replaced by \mathbf{I}^1 norms. This is however not enough to specify the geometry of large amplitude wavelet coefficients. Scattering transforms provide information about this geometry by computing interaction terms across scales, with an iterated wavelet transform. Their mathematical properties are described in [26, 10], and applications to image and audio classification are studied in [9, 2]. We review important properties needed to define microcanonical models.

Wavelets are optimized in order to build sparse signal representations. For audio signals in dimension $\ell = 1$, each wavelet is a complex filter whose Fourier transform $\hat{\psi}_q(\omega)$ has an energy concentrated in the interval $[2^{q/Q}, 2^{(q+1)/Q}]$. The parameter Q is the number of wavelets per octave, which adjusts their frequency resolution. Sparse representations of audio signals are obtained with about $Q = 24$ wavelets per octave, which are similar to half-tone musical notes. In numerical computations, we choose Gabor wavelets as in [2].

For images in $\ell = 2$ dimensions, each wavelet is computed by rotating a single mother wavelet $\psi_q(u) = \psi(r_q^{-1}u)$ where $r_q u$ is a rotation of $u \in \mathbb{R}^2$ by an angle $q\pi/Q$. Wavelet

coefficients $x \star \psi_{j,q}$ compute variations of x at scales 2^j along different directions. In this case, Q is the angular resolution of each wavelet. In numerical computations we use Morlet wavelets as in [9].

The modulus of wavelet coefficients $|x \star \psi_{j,q}(u)|$ specifies the variability of x at different scales, around its mean over a cube $u \in \Lambda_d$: $d^{-1} \sum_{u \in \Lambda_d} x(u)$. A normalized \mathbf{I}^1 norm computes the average of $|x \star \psi_{j,q}(u)|$

$$d^{-1} \|x \star \psi_{j,q}\|_1 = d^{-1} \sum_{u \in \Lambda_d} |x \star \psi_{j,q}(u)| .$$

To capture this intermittency which specifies the geometry of large amplitude coefficients, a scattering transform measures the multiscale variability of $|x \star \psi_{j,q}(u)|$ through convolutions with a new set of wavelets. For simplification, we shall consider here that the new wavelets are identical to the first ones, although they may be changed as in [2]:

$$||x \star \psi_{j,q} \star \psi_{j',q'}(u)|.$$

The maximum scales 2^j and $2^{j'}$ remain below a cut-off scale 2^J which specifies the maximum interaction range of the model. Incorporating first and second order coefficients defines a new potential which captures the multiscale variations of x as well as interaction terms across scales:

$$Ux = \{x, |x \star \psi_{j,q}|, ||x \star \psi_{j,q} \star \psi_{j',q'}||\}_{j,j' \leq J, q, q' \leq Q}. \quad (43)$$

The corresponding energy vector is

$$\Phi_d x = \left\{ d^{-1} \sum_{u \in \Lambda_d} x(u), d^{-1} \|x \star \psi_{j,q}\|_1, d^{-1} \| |x \star \psi_{j,q} \star \psi_{j',q'}| \|_1 \right\}_{j,j' \leq J, q, q' \leq Q} . \quad (44)$$

It includes $K = 1 + JQ + J^2Q^2$ coefficients. If the wavelets satisfy the Littlewood Paley inequality (38) then one can prove [26] that the scattering operator Φ_d is contracting for any x and x' in I^{Λ_d} :

$$\|\Phi x - \Phi x'\|_2 \leq \|x - x'\|_2 .$$

Indeed, as in (39), one can show that (38) implies that $\overline{W}x = \{d^{-1} \sum_u x(u), x \star \psi_{j,q}\}_{j \leq J, q \leq Q}$ is a contractive operator. The operator Φ_d can be computed by iterating twice on the operator \overline{W} and on the modulus non-linearity which is also contractive. A product of contractions is a contraction so Φ_d is a contraction.

An important property of wavelet \mathbf{I}^p norms is their stability to deformations. A small deformation of $x(u)$, if u is a continuous variable, is the action of a small diffeomorphism on x which yields $x_\tau(u) = x(u - \tau(u))$ where $\tau(u)$ is a \mathbf{C}^1 function with $\|\nabla \tau\|_\infty < 1$. Small deformations typically occur over images and other physical phenomena, so we expect that probability measures are Lipschitz continuous to actions of diffeomorphisms. To build microcanonical models which are stable to deformations, the interaction energy must also be Lipschitz continuous to actions of diffeomorphisms. This is proved for wavelet interaction energies [26] because multiscale separations provide stability to deformations.

Sparsity conditions We now show that these \mathbf{l}^1 norms can capture the geometry of positive point processes obtained as sums of Diracs. If $x \geq 0$ then $\sum_{u \in \Lambda_d} x(u) = \|x\|_1$ is also a sparsity measure. Young's inequality implies that

$$\|x \star \psi_{j,q}\|_1 \leq \|x\|_1 \|\psi_{j,q}\|_1.$$

If x is a Dirac in Λ_d then this inequality is an equality. Conversely, the following theorem proves that if this inequality is an equality then x is highly sparse.

Theorem 4.1. *Let $\varphi_q(u)$ be the complex phase of $\psi_q(u)$. Suppose that $|\psi_q(u)| > 0$ for $u \in [-\alpha, \alpha]^\ell$ and that there exists $\xi_q \in \mathbb{R}^\ell$ and $\beta > 1$ such that*

$$\beta^{-1} |\xi_q \cdot (u - u')| \leq |\varphi_q(u) - \varphi_q(u')| \leq \beta |\xi_q \cdot (u - u')|. \quad (45)$$

If $\|x \star \psi_{j,q}\|_1 = \|x\|_1 \|\psi_{j,q}\|_1$ then either $\xi_q \cdot (u - u') = 0$ or

$$|\xi_q \cdot (u - u')| \geq C 2^j \quad \text{with } C = \min(\pi \beta^{-1}, 2\alpha |\xi_q|). \quad (46)$$

In dimension $\ell = 1$ then wavelets are dilated and we have $\psi_q(u) \approx 2^{-q/Q} \psi(2^{-q/Q} u)$. We usually choose $\psi(u)$ to be a wavelet with a linear phase in which case $\beta = 1$ in (45). If $\|x \star \psi_{j,q}\|_1 = \|x\|_1 \|\psi_{j,q}\|_1$ then Theorem 4.1 proves in (46) that x is a sum of isolated Diracs whose distances are larger than $C 2^j$.

In dimension $\ell = 2$ then wavelets are also rotated and $\psi_q(u) = \psi(r_q^{-1} u)$. We usually choose a linear phase so $\phi_q(u) = r_q \xi \cdot u$ where ξ then normalized horizontal vector in \mathbb{R}^2 . It follows that $\xi_q = r_q \xi$ is a vector of angle $q\pi/Q$ in \mathbb{R}^2 . In this case, Theorem 4.1 proves in (46) that the support of x is included in straight lines perpendicular to ξ_q , and hence of angular direction $q\pi/Q + \pi/2$, and whose distances are larger than $C 2^j$.

5 Numerical Results

This section compares microcanonical models for different stationary processes and different interaction energy vectors Φ_d . Microcanonical models aim at estimating high-dimensional probability densities which are often unknown. Evaluating the precision of such model is thus a major challenge. We review required concentration properties and introduce a numerical evaluation which compares models through errors produced by estimators conditioned on these models.

Section 2.1 explains that one can approximate the distribution of X with a microcanonical model calculated from Φ_d only if $\Phi_d X$ converges to $\mathbb{E}(\Phi_d X)$ with probability 1 when d goes to ∞ . If $\|\mathbb{E}(\Phi_d X)\|$ is uniformly bounded then this is obtained if

$$\lim_{d \rightarrow \infty} \mathbb{E}(\|\Phi_d X - \mathbb{E}(\Phi_d X)\|^2) = 0.$$

This is a first test which can be evaluated empirically from realizations of X .

This condition implies that realizations of X concentrate in microcanonical sets Ω_{d,ϵ_d} for an ϵ_d which converges to 0 with a probability which tends to 1, when d goes to ∞ . These sets may however be too large and hence define microcanonical models $X_{d,\epsilon}$ whose entropy is much larger than the entropy of X . For Ising processes studied in the next section, the density $p(x)$ is known so the model can be evaluated by verifying that $-\mathbb{E}(\log p(X_{d,\epsilon}))$ remains close to the entropy $-\mathbb{E}(\log p(X))$. However, for many complex processes such as turbulence, image or audio textures, the density p is unknown. For image and audio textures, perceptual evaluations can be used to evaluate the model precision. If the entropy of the microcanonical model $X_{d,\epsilon}$ is too large, it does not reproduce typical perceptual structures of an image or an audio texture X .

5.1 Ising Process

We consider a two-dimensional Ising process with no outside magnetization, over a two-dimensional square lattice with periodic boundary conditions. The spin values of $x(u)$ take their values in $\{-1, 1\}$ and the Ising probability of x is

$$p(x) = \mathcal{Z}^{-1} \exp(-\beta H_I(x)) \text{ with } H_I(x) = d^{-1} \sum_{u \in \Lambda_d} \sum_{u' \in \mathcal{N}_u} x(u)x(u'), \quad (47)$$

where \mathcal{N}_u is the 4 point neighborhood of $x(u)$ in the two-dimensional grid and $\beta = (k_B T)^{-1}$ is a reciprocal of the temperature of the system scaled by the Boltzmann constant k_B . This model has been extensively studied since the work of Onsager [28]. It has a phase transition when T reaches a critical value $T_c \approx 2.27$. We study the approximation of Ising for several values of the temperature. Observe that $x(u)x(u') = 1 - |x(u) - x(u')|^2/2$ so

$$\sum_{u \in \Lambda_d} \sum_{u' \in \mathcal{N}_u} x(u)x(u') = x(u)x(u') = d - 2^{-1} \sum_{u \in \Lambda_d} \sum_{u' \in \mathcal{N}_u} |x(u) - x(u')|^2. \quad (48)$$

The right hand-side term is the \mathbf{l}^2 norm of discretized gradient of x .

We study the approximation of the Ising model with a wavelet energy vector defined over configurations $x \in I^{\Lambda_d}$ with $I = [-1, 1]$. Suppose that $x(u)$ is a function defined over $u \in \mathbb{R}^2$ with $\int_{\mathbb{R}^2} |\nabla x(u)|^2 du < \infty$. The equivalence between Sobolev norms and weighted norms over wavelet coefficients proves that for appropriate wavelets

$$\int_{\mathbb{R}^2} |\nabla x(u)|^2 du \sim \sum_{j \in \mathbb{Z}} \sum_q 2^{-2j} \|x \star \psi_{j,q}\|_2^2.$$

The Ising Hamiltonian (48) on a discrete grid can thus be approximated with discrete wavelet \mathbf{l}^2 norms up to a maximum scale $j \leq J$. This multiscale representation is intimately related to the Renormalization Group, which has been successfully applied to analyse the two-dimensional Ising model [21]. We impose that $x \in I^{\Lambda_d}$ by computing a sliced wavelet

energy vector, with a single slice calculated with the sigmoid $\sigma(t) = (1 + e^{-\frac{t}{\eta}})^{-1}$ for a small value of η , ensuring that the samples from the model satisfy $x(u) \in [-1, 1]$. Also, observe that if $x(u) \in I = [-1, 1]$ for all u , then

$$|x| \equiv 1 \Leftrightarrow \|x\|_2^2 = d,$$

therefore by adding $\|x\|_2^2$ into the energy vector Φ_d , we characterize the fact that x is a binary vector.

Since by definition the Ising model is the maximum entropy distribution conditioned on its expected Hamiltonian $H_I(x)$ in (47) over $\{-1, 1\}^{\Lambda_d}$, one can define a microcanonical interaction energy $\Phi_d(x) = \{H_I(x), \|x\|^2\}$, for $x \in [-1, 1]^{\Lambda_d}$, which converges to the true Ising model in the limit $d \rightarrow \infty$ by the Boltzmann equivalence principle. However, as explained in Section 3.3, the performance of the microcanonical gradient descent sampling can be improved by adding additional energy components that improve the convergence towards the microcanonical set. Table 1 shows the empirical concentration of $\Phi_d(x)$ for Ising models at varying temperatures, for several choices of scale. The Ising model has a phase transition at the critical temperature $T_c \approx 2.27$, from an ‘ordered’ to a ‘disordered’ state. The spin spatial correlation exhibits a characteristic scale away from T_c $\mathbb{E}\{X(u)X(u+r)\} \simeq e^{-|r|/\xi(T)}$, and is self-similar at $T = T_c$: $\mathbb{E}\{X(u)X(u+r)\} \simeq |r|^{-1/2}$.

Table 1 shows that despite the presence of long-range correlations nearby T_c , the energy vector $\Phi_d X$ has strong concentration, justifying the corresponding microcanonical approximation. As described in Section 2.4, this concentration ensures that typical samples from the true distribution will be included in the typical set of the corresponding microcanonical measure, but the reciprocal requires that the microcanonical sets adapt to the level sets of the original density.

Using Onsager’s analytic solution, we can compute the free energy $\log \mathcal{Z}$ and therefore estimate the cross-entropy $\widehat{\mathbb{E}}_{X \sim p_{d,\epsilon}}[-\log p(X)]$ of the microcanonical approximation for several choices of Φ_d . Table 2 reports the values of estimated cross-entropy obtained from samples of the microcanonical measure. The multiscale microcanonical gradient descent significantly outperforms the direct microcanonical approximation for sufficiently large J , confirming that the gradient descent is “renormalized” by adding constraints at different scales. The mathematical analysis of such renormalization phenomena is however beyond the scope of this paper.

Figure 1 shows samples from the microcanonical model under several choices of energy vector and temperature. We verify that at low temperature, the long-range correlations are significant, and are appropriately captured when the microcanonical model contains wavelets at sufficiently large scale. The direct microcanonical approximation defines an optimization landscape with poor convergence towards the microcanonical set. It appears much more clearly by looking at realizations of the resulting microcanonical process than from cross entropy measures.

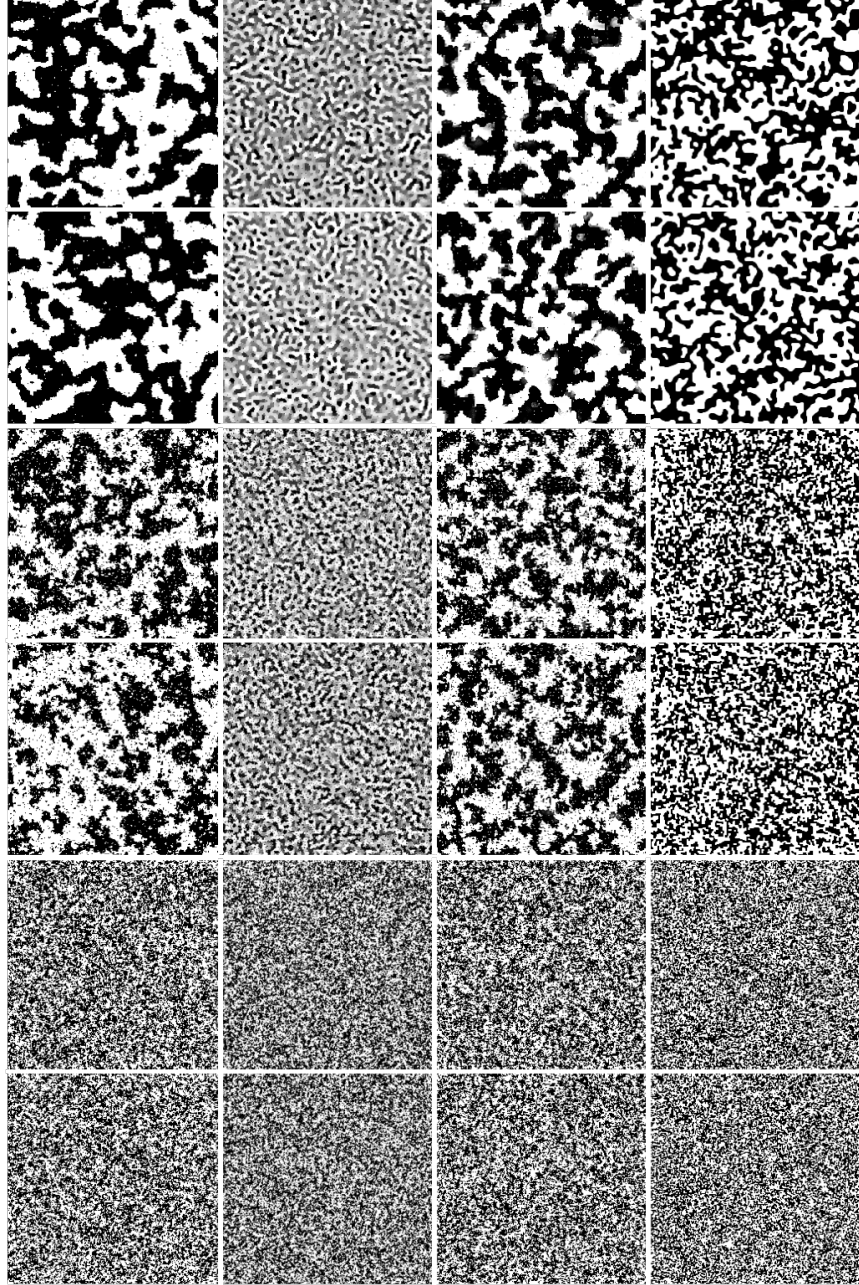


Figure 1: Examples of Ising samples at temperatures $T = 1.4$ (top), $T = 2.2 \approx T_c$ (center) and $T = 3.8$ (bottom). We display two independent samples on each row. From left to right: (i) original canonical model, (ii) scattering model with $J = 3$ (iii) scattering model with $J = 6$, (iv) microcanonical model using the Ising sufficient statistics.

Temp	Scat. $J = 3$	Scat. $J = 6$	$\Phi_d(x) = H_I(x)$
1.4	1.6e-5	5e-5	2e-5
$2.2 \approx T_c$	1.4e-5	3.7e-5	1e-5
3	5e-6	8e-6	2e-6
3.8	3e-6	5e-6	1e-6

Table 1: Empirical Normalized Variance $\frac{\widehat{\mathbb{E}}\{\|\Phi_d(x) - \widehat{\mathbb{E}}\Phi_d(x)\|^2\}}{\|\widehat{\mathbb{E}}\Phi_d(x)\|^2}$ for different settings of Ising temperature and wavelet scattering representation. We used samples of size $d = 512^2$.

Temp	Scat. $J = 3$	Scat. $J = 6$	$\Phi_d(x) = H_I(x)$	Entropy
1.4	$0.34 \pm 4\text{e-}3$	$0.32 \pm 2\text{e-}2$	$0.44 \pm 7\text{e-}3$	0.32
2.2	$0.61 \pm 2\text{e-}3$	$0.59 \pm 8\text{e-}3$	$0.62 \pm 6\text{e-}3$	0.59
3	$0.85 \pm 2\text{e-}3$	$0.85 \pm 5\text{e-}4$	$0.84 \pm 4\text{e-}3$	0.84
3.8	$0.86 \pm 4\text{e-}4$	$0.86 \pm 5\text{e-}4$	$0.85 \pm 2\text{e-}3$	0.85

Table 2: Estimated Cross-Entropy $\widehat{\mathbb{E}}_{X \sim p_{d,\epsilon}} -\log p(X)$ for different choices of microcanonical models.

5.2 Cox processes convolved with patterns

Point processes provide powerful models of stochastic geometry, with applications in many areas of astrophysics, neuroscience, finance and computer vision. A point process N on \mathbb{R}^ℓ is a measure whose support is composed of isolated points. Second-order point processes [7] are those satisfying $\mathbb{E}[N(C)^2] < \infty$ for all bounded Borel sets $C \subset \mathbb{R}^\ell$. If N is a stationary, second-order point process, one can define its associated Bartlett spectral measure [7] μ_N , which generalizes the power spectrum of second-order stationary processes.

Given a non-negative stationary process $\lambda(t)$, $t \in \mathbb{R}^\ell$, a Cox process N is defined as a Poisson process conditional on λ with intensity $\lambda(t)$. Important geometric information of N is captured by its Bartlett power spectrum, which satisfies $\mu_N(d\omega) = \mu_\lambda(d\omega) + \mathbb{E}\lambda \delta(d\omega)$ [7]. Large classes of random processes are constructed as convolutions of point processes with some filter $h(t)$

$$X(t) = N \star h(t) , \quad h \in L^1(\mathbb{R}^\ell) \cap L^2(\mathbb{R}^\ell) .$$

The filter $h(t)$ can be interpreted as a pattern which is randomly translated at point locations and added. It may also be the transfer function of a detector measuring the point-process. In this case, the power spectrum of X is $\mu_X(d\omega) = \mu_N(d\omega)|\hat{h}(\omega)|^2$, which mixes the geometric information of N with the profile of the filter h .

This loss of information is due to the fact that the power spectrum does not measure scale interactions. When there is a scale separation between N and h , ie

$$(\mathbb{E}\lambda)^2 \gg \int u^2 |h(u)|^2 du \quad (49)$$

	$J = 2$		$J = 4$		$J = 6$	
	σ^2	$\Phi_d^\#$	σ^2	$\Phi_d^\#$	σ^2	$\Phi_d^\#$
$m = 1$	1.2e-6	21	1.4e-6	38	1.5e-6	52
$m = 2$	1.3e-6	88	1.7e-6	422	1.8e-6	580

Table 3: Empirical normalized variance $\sigma^2 = \frac{\widehat{\mathbb{E}}\{\|\Phi_d(x) - \widehat{\mathbb{E}}\Phi_d(x)\|^2\}}{\|\widehat{\mathbb{E}}\Phi_d(x)\|^2}$ and number of coefficients $\Phi_d^\#$ of scattering representation for different order m and scale 2^J . We used samples of size $d = 256^2$.

then for sufficiently small scales j , one can verify [10] that

$$|X \star \psi_{j,q}| = |N \star (\psi_{j,q} \star h)| \approx N \star |\psi_{j,q} \star h| \quad (50)$$

with high probability, due to the fact that the events in N rarely interact at spatial scales j such that $2^j \ll \mathbb{E}\lambda$. From this approximation, it follows that for sufficiently large scale gap $j' \gg j$, we have

$$||X \star \psi_{j,q}| \star \psi_{j',q'}| \approx C_{j,q} |N \star \psi_{j',q'}|, \quad (51)$$

since $|\psi_{j,q} \star h| \star \psi_{j',q'} \approx C_{j,q} \delta \star \psi_{j',q'}$. Second order scattering coefficients, indexed with pairs (j, q, j', q') , thus provide measurements that convey spectral information about the point process N as (j', q') varies, disentangled from the spectral information of h .

We illustrate this phenomena by considering a two-dimensional Cox point process $N(u)$, whose rate $\lambda(u)$ is a stationary Gaussian process whose power spectrum is concentrated in the low-frequencies, and with an integral scale of 100 pixels. This Cox process is convolved with a pattern $h(u)$ with zero mean and small spatial support of 5 pixels. Table 3 reports empirical variance results for different choices of maximum scale (J) and scattering order (m). Because $X(u)$ does not exhibit long-range dependencies, we verify that the scattering coefficients quickly concentrate around their mean, enabling micro-canonical approximations. Figure 2 displays samples from the microcanonical scattering model using different choices of representation. We observe that, as predicted, first-order coefficients alone do not capture the different properties of the point process and of the filter. The microcanonical model generates a Gaussian-like fields whose power spectra mixes both sources. On the other hand, as soon as the scattering maximum scale 2^J reaches the characteristic scale of N , the second order microcanonical scattering model can restore both the characteristic geometry of N and the profile of h and hence provides more accurate stochastic model.

This simple example motivates the need to consider generalized moments in order to model random fields with complex geometric structure, such as textures. Next section explores the ability of scattering microcanonical models to synthesize generic image, audio and turbulence textures.

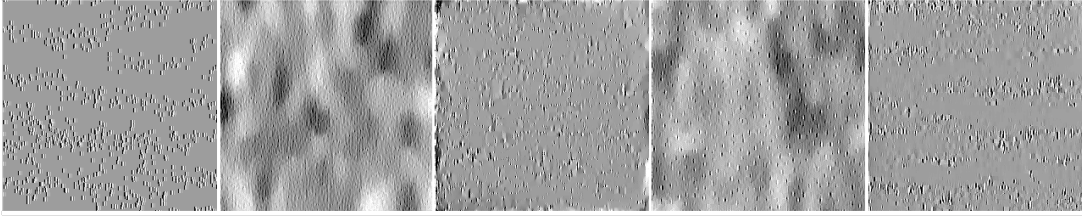


Figure 2: Samples from microcanonical model for different choice of scattering representations. *from left to right*: original, $(m = 1, J = 3)$, $(m = 1, J = 6)$, $(m = 2, J = 3)$, $(m = 2, J = 6)$.

5.3 Image and Audio Textures

An image or audio texture is the realization of a stationary process. Textures synthesis amounts to compute signals which are perceptually nearly identical to a given texture. The quality of a texture model is thus evaluated from a perceptual point of view. We review previous work and give results obtained with a scattering microcanonical model.

Geman and Geman [20] have introduced macrocanonical models based on Markov random fields, which provide good texture models as long as these textures are realizations of random processes having no long range correlation. Several approaches have then been introduced to incorporate long range correlations. Heeger and Bergen [22] capture texture statistics through the marginal distributions obtained by filtering images with oriented wavelets. This approach has been generalized by the macrocanonical Frame model of Mumford and Zhu [36], based on marginal distributions of filtered images. The Cramer-Wold theorem proves that the d -dimensional joint probability distribution of X in Λ_d is characterized by the one-dimensional probability densities of linear combinations $\langle X, a \rangle = \sum_{u \in \Lambda_d} X(u) a(u)$ for all $a \in \mathbb{R}^{\Lambda_d}$. One can write such linear combinations as convolutions $X \star h(u)$, but Cramer-Wold theorem requires to use all filters $h \in \mathbb{R}^{\Lambda_d}$. Inspired by this result, Mumford and Zhu [36] have introduced a maximum entropy canonical models from limited sets of J optimized filters $\{h_j\}_{j \leq J}$. The probability densities of $X \star h_j$ are approximated by maximum entropy distributions conditioned by marginals probability density of $X \star \phi_j$, estimated over non-overlapping quantization intervals I_m . However, these approaches have been limited by the rapid growth of the dimensionality of the resulting interaction energy vector Φ_d , which is the product $J \times M$ of the number of filters by the number of quantization bins.

Portilla and Simoncelli [30] made important improvements to these texture models, with wavelet transforms. They capture the correlation of the modulus of wavelet coefficients with a covariance matrix computed over a fixed range M . Although they refer to a macrocanonical maximum entropy formalism, their computations rather correspond to a microcanonical estimation, where the synthesis is performed with alternate projections on the model constraints. If calculated over J scales, the energy vector Φ_d has $O(JM^2)$

$m = 1$	$m = 2$
1.4e-16 (38)	3e-15 (550)

Table 4: Empirical Normalized Variance $\frac{\widehat{\mathbb{E}}\{\|\Phi_d(x) - \widehat{\mathbb{E}}\Phi_d(x)\|^2\}}{\|\widehat{\mathbb{E}}\Phi_d(x)\|^2}$ and size of scattering representations for different orders. We use $J = 6$, and samples of size $d = 256^2$.

coefficients. This approach was extended to audio textures by McDermott and Simoncelli [27]. A scattering representation is closely related to Portilla and Simoncelli model since it also computes the modulus of wavelet coefficients, but it replaces covariance measurements by multiscale ℓ^1 norms computed with a second order wavelet transform. The resulting representation has $O(J^2)$ coefficients as opposed to $O(JM^2)$.

The modeling capacity of wavelet marginal models have been increased with translation-invariant representation arising from deep convolutional neural networks. In [19], the authors consider a deep VGG convolutional network, trained on a large-scale image classification task. They construct an interaction energy vector $\Phi_d(X)$ which is a channel cross-correlation of feature maps at every layer of the VGG networks. With a gradient descent microcanonical sampling algorithm, the authors have obtained excellent visual texture synthesis. However, the dimension of the energy vector $\Phi_d(X)$ is larger than the dimension d of X and thus does not concentrate well. Although synthesis are of good visual quality, these estimators are not statistically consistent and have no asymptotic limit. Such algorithms have a tendency to restore random processes of lower entropy than the original process, by overspecifying the model with more parameters than the signal dimension.

Comparing different texture models depends on the application goal. Best image quality is obtained with convolutional neural network approaches which use a large number of parameters. However, these models do not seem to provide consistent models of probability measures of stochastic processes. Scattering representations are mathematically simpler and involve a number of coefficients which does not increase with the dimensionality d . We show that the scale interaction terms are able to capture important geometrical texture structures although the resulting images do not have the visual quality of deep neural network models.

In the following, we give results of scattering microcanonical model on a collection of natural image and auditory textures. The Brodatz image texture dataset ¹ consists of 155 texture classes, with a single 512×512 sample per class. Auditory textures are taken from McDermott and Simoncelli [27], which contains 1 second samples of different sounds.

Figure 3 displays original textures and synthesis obtained from different microcanonical models, and Table 4 gives the empirical variance of the scattering representation, estimated from the available samples on a subset of texture classes. Empirical scattering coefficients quickly concentrate, as a result of the ergodic properties of most textures from the sample

¹Available at <http://sipi.usc.edu/database/database.php?volume=textures>

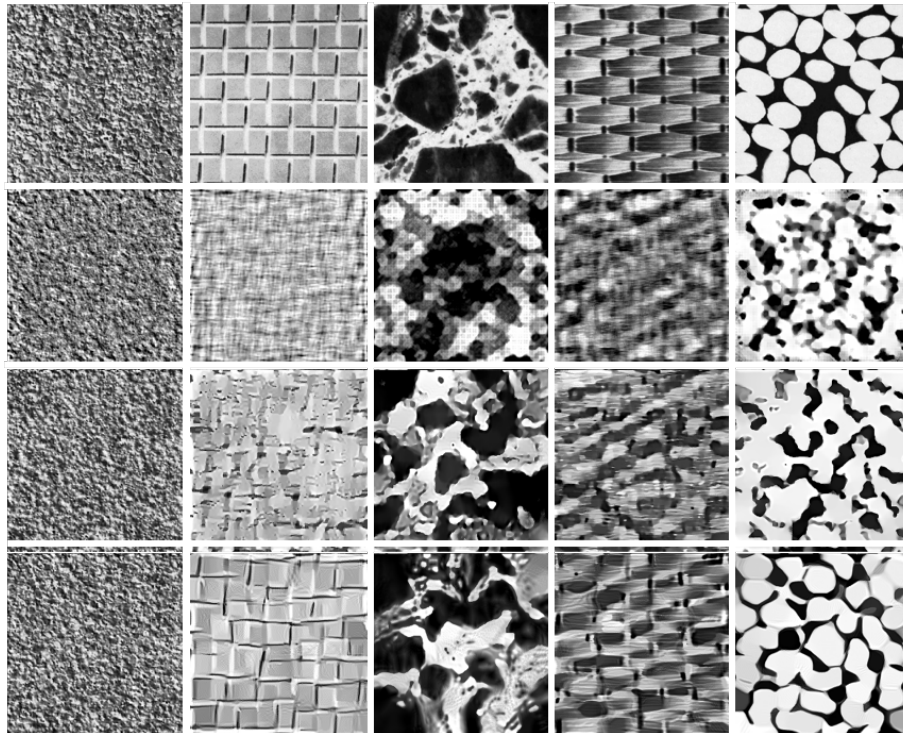


Figure 3: Examples of texture Synthesis. Image rows from top to bottom display: original images , wavelet l^2 norm models, wavelet l^1 norm models, second order scattering models.

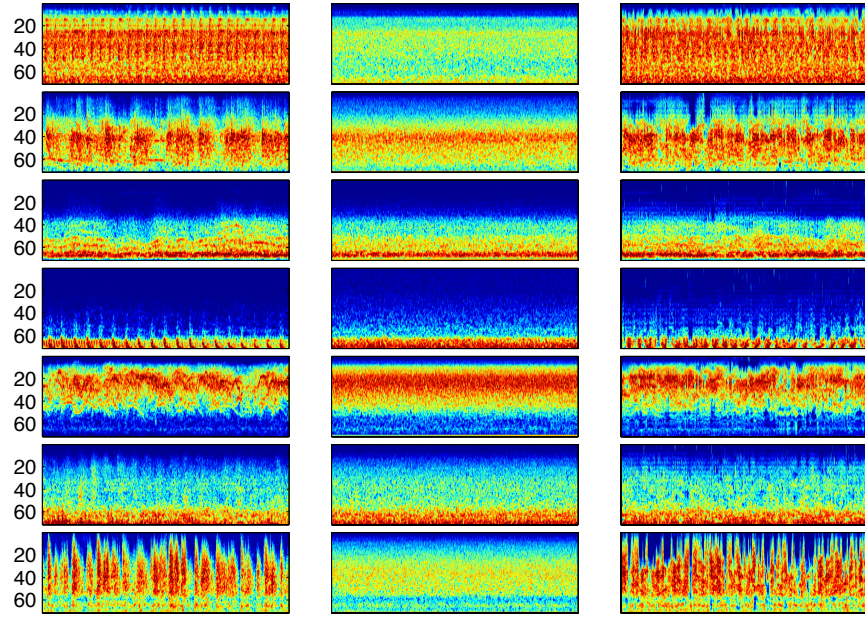


Figure 4: Examples of audio texture synthesis. These images display the spectrogram of each audio signal. The left, middle and right columns correspond to original signals, l^2 norm wavelet models, and second order scattering models.

set. Reconstructions using \mathbf{l}^2 wavelet norms are typical samples from Gaussian random fields whose power spectra is matched within each wavelet sub-band according to (42). First order scattering coefficients are wavelet \mathbf{l}^1 norms which provide multiscale sparsity information. However, second order coefficients are needed to restore good approximations of texture geometries.

The reconstruction of auditory textures is performed with a complex wavelet representation [8]. Auditory textures have a rich mixture of homogeneous and impulsive, transient components, as well as amplitude and frequency modulation phenomena. Figure 4 displays the spectrograms of original auditory textures, together with reconstructions from \mathbf{l}^2 norms of wavelet coefficients and reconstructions from second order scattering coefficients. Whereas \mathbf{l}^2 models are unable to capture such non-gaussian phenomena, second order scattering coefficients provide an efficient and compact representation that restores amplitude and frequency modulations.

6 Conclusion

Consistent density estimation in the high-dimensional regime requires exploiting regularity priors in order to beat the curse of dimensionality. Microcanonical ensembles provide a framework that consistently approximates maximum entropy distributions under ergodicity assumptions, such as absence of long-range correlations. The resulting models are efficiently estimated, and gradient descent provides an approximate sampling algorithm that replaces standard MCMC tools. This paper presents a mathematical framework to study both the statistical and algorithmic aspects of such microcanonical density models.

Many physical phenomena is non-Gaussian, but exhibits local regularity that can be exploited with \mathbf{l}^1 wavelet microcanonical models, that capture such regularity through the sparsity of the resulting wavelet coefficients. Although wavelet sparsity is a powerful statistical model, it is unable to account for the scale and orientation interactions that define most complex geometric structures. We showed that second order scattering coefficients can be used to capture such interactions in several synthetic and real examples.

Despite these initial steps, our current analysis still presents several important limitations. First, our convergence analysis does not currently cover many practically interesting cases, and the relationship with other algorithms such as Herding and Hamilton Monte-Carlo deserves further investigation. Next, scattering microcanonical models and its corresponding sampling algorithm are closely related to recent state-of-the-art texture synthesis using Convolutional Neural Networks. Understanding the tradeoffs of learning microcanonical energies rather than designing them with multiscale wavelets is another major direction of future research.

References

- [1] Pierre-Antoine Absil, Robert Mahony, and Benjamin Andrews. Convergence of the iterates of descent methods for analytic cost functions, 2004.
- [2] J. Anden and S. Mallat. Deep scattering spectrum. *Submitted to IEEE transactions of Signal Processing*, 2013.
- [3] F. Barthe, O. Guédon, S. Mendelson, and A. Naor. A probabilistic approach to the geometry of l_p^n -ball. *Ann. Probab.*, 33(2):480–513, 2005.
- [4] G. Battle. *Wavelets and Renormalization*. World Scientific, Singapore, 1998.
- [5] Michael Betancourt. A conceptual introduction to hamiltonian monte carlo. *arXiv preprint arXiv:1701.02434*, 2017.
- [6] E. Borel. Sur les principes de la theorie cinetique des gas. *Ann. de l'Ecole Norm. Sup.*, 23:9–33, 1906.
- [7] Pierre Brémaud, Laurent Massoulié, Andrea Ridolfi, and Fédérale Lausanne Epfl. Power spectra of random spike fields & related processes. In *Journal of Applied Probability*. Citeseer, 2003.
- [8] Joan Bruna and Stéphane Mallat. Audio texture synthesis with scattering moments. *arXiv preprint arXiv:1311.0407*, 2013.
- [9] Joan Bruna and Stéphane Mallat. Invariant scattering convolution networks. *IEEE transactions on pattern analysis and machine intelligence*, 35(8):1872–1886, 2013.
- [10] Joan Bruna, Stéphane Mallat, Emmanuel Bacry, Jean-François Muzy, et al. Intermittent process analysis with scattering moments. *The Annals of Statistics*, 43(1):323–351, 2015.
- [11] James V Burke, Adrian S Lewis, and Michael L Overton. A robust gradient sampling algorithm for nonsmooth, nonconvex optimization. *SIAM Journal on Optimization*, 15(3):751–779, 2005.
- [12] Sourav Chatterjee. A note about the uniform distribution on the intersection of a simplex and a sphere. *Journal of Topology and Analysis*, 9(04):717–738, 2017.
- [13] Michael Creutz. Microcanonical monte carlo simulation. *Physical Review Letters*, 50(19):1411, 1983.
- [14] A. Dembo and O. Zeitouni. *Large Deviations Techniques and Applications*. Johns and Bartett Publishers, Boston, 1993.

- [15] J.D. Deuschel, D. Stroock, and H. Zessin. Microcanonical distributions for lattice gases. *Commun. Math. Phys.*, 139:83–101, 1991.
- [16] P. Diaconis and D. Freedman. A dozen de finetti-style results in search for a theory. *Ann. Inst. Poincaré*, 23:417–433, 1987.
- [17] M. D. Dosker and S. R. S. Varadhan. Large deviations for stationary gaussian processes. *Commun. Math. Phys.*, 97:187–210, 1985.
- [18] Isabelle Gallagher, Laure Saint-Raymond, and Benjamin Texier. From newton to boltzmann: hard spheres and short-range potentials. *arXiv preprint arXiv:1208.5753*, 2012.
- [19] Leon Gatys, Alexander S Ecker, and Matthias Bethge. Texture synthesis using convolutional neural networks. In *Advances in Neural Information Processing Systems*, pages 262–270, 2015.
- [20] Stuart Geman and Donald Geman. Stochastic relaxation, gibbs distributions, and the bayesian restoration of images. *IEEE Transactions on pattern analysis and machine intelligence*, (6):721–741, 1984.
- [21] Hans-Otto Georgii. *Gibbs Measures and Phase Transitions*. Walter de Gruyter, Berlin, 2011.
- [22] David J Heeger and James R Bergen. Pyramid-based texture analysis/synthesis. In *Proceedings of the 22nd annual conference on Computer graphics and interactive techniques*, pages 229–238. ACM, 1995.
- [23] Edwin T Jaynes. Information theory and statistical mechanics. *Physical review*, 106(4):620, 1957.
- [24] Ross Kindermann and J Laurie Snell. *Markov random fields and their applications*, volume 1. American Mathematical Society, 1980.
- [25] Jason D Lee, Max Simchowitz, Michael I Jordan, and Benjamin Recht. Gradient descent only converges to minimizers. In *Conference on Learning Theory*, pages 1246–1257, 2016.
- [26] Stéphane Mallat. Group invariant scattering. *Communications on Pure and Applied Mathematics*, 65(10):1331–1398, 2012.
- [27] Josh H McDermott and Eero P Simoncelli. Sound texture perception via statistics of the auditory periphery: evidence from sound synthesis. *Neuron*, 71(5):926–940, 2011.
- [28] Lars Onsager. Crystal statistics. i. a two-dimensional model with an order-disorder transition. *Physical Review*, 65(3-4):117, 1944.

- [29] Ioannis Panageas and Georgios Piliouras. Gradient descent converges to minimizers: The case of non-isolated critical points. *CoRR*, abs/1605.00405, 2016.
- [30] Javier Portilla and Eero P Simoncelli. A parametric texture model based on joint statistics of complex wavelet coefficients. *International journal of computer vision*, 40(1):49–70, 2000.
- [31] Alexander Sokol. Advanced Probability (Lecture Notes), 2013.
- [32] D. W. Stroock and O. Zeitouni. Microcanonical distributions, gibbs states and the equivalence of ensembles. *Random Walks, Brownian Motion, and Interacting PARTICLE Systems*, pages 399–424, 1991.
- [33] Martin J Wainwright, Michael I Jordan, et al. Graphical models, exponential families, and variational inference. *Foundations and Trends® in Machine Learning*, 1(1–2):1–305, 2008.
- [34] Yu Wang, Wotao Yin, and Jinshan Zeng. Global convergence of admm in nonconvex nonsmooth optimization. *arXiv preprint arXiv:1511.06324*, 2015.
- [35] Max Welling. Herding dynamical weights to learn. In *Proceedings of the 26th Annual International Conference on Machine Learning*, pages 1121–1128. ACM, 2009.
- [36] Song Chun Zhu, Yingnian Wu, and David Mumford. Filters, random fields and maximum entropy (frame): Towards a unified theory for texture modeling. *International Journal of Computer Vision*, 27(2):107–126, 1998.

A Proof of Theorem 3.1

A.1 Proof of part (i)

The main technical challenge to prove (26) is to show that assumption (C) is sufficient to guarantee that $|J\Phi_d x|^{-1}$ is integrable. Since Φ_d is Lipschitz from assumption (A), the coarea formula proves that for any integrable function $g(x)$

$$\int_B g(x) |J\Phi_d x| dx = \int_{\mathbb{R}^K} \int_{\Phi_d^{-1}(y)} g(x) d\mathcal{H}^{d-K}(x) dy . \quad (52)$$

In order to apply (52) to $H(p_{d,\epsilon}^y)$, we need to show that $|J\Phi_d(x)|^{-1}$ is integrable in $\Phi_{d,\epsilon}^{-1}(y)$. Using the notation for each Jacobian column (22), we verify that $|J\Phi_d(x)|$ satisfies

$$|J\Phi_d(x)| \geq \max \{ |\det[\bar{J}U(\bar{X}_1), \dots, \bar{J}U(\bar{X}_K)]|, \dots, |\det[\bar{J}U(\bar{X}_{\bar{d}+1}), \dots, \bar{J}U(\bar{X}_{\bar{d}+K})]| \} , \quad (53)$$

where \bar{X}_i is a projection of x onto disjoint subsets of $2\Delta + 1$ coordinates, and $\tilde{d} \geq d(2\Delta + 1)^{-1} = \Theta(d)$.

We will show that for d large enough and arbitrary $R > 0$,

$$\int_{|x|_\infty < R} |J\Phi_d(x)|^{-1} dx < \infty, \quad (54)$$

by interpreting (54) as proportional to the expected value of $\mathbb{E}_{X \sim \text{Unif}(d, R)} |J\Phi_d(X)|^{-1}$. Since $\Phi_{d, \epsilon}^{-1}(y)$ is a compact set thanks to assumption (B), it is bounded, so $\Phi_{d, \epsilon}^{-1}(y) \subseteq \{x; |x|_\infty < R\}$ for some R , which proves that $|J\Phi_d(x)|^{-1}$ is integrable in $\Phi_{d, \epsilon}^{-1}(y)$.

For that purpose, let us prove that assumption (C) from eq (25) is sufficient to guarantee (54). We first observe that thanks to (53), if Y denotes the random variable $Y = |\det[\bar{J}U(\bar{X}_1), \dots, \bar{J}U(\bar{X}_K)]|$ and $F_Y(y)$ is its cumulative distribution function, it is sufficient to show that

$$F_Y(y) \simeq y^\eta, \text{ for some } \eta > 0, (y \rightarrow 0). \quad (55)$$

Indeed, since $V = |J\Phi_d(X)| \geq \max(Y_1, \dots, Y_{\tilde{d}})$ with Y_i independent and identically distributed, we have that

$$F_V(y) \leq F_Y(y)^{\tilde{d}} \simeq y^{\eta \tilde{d}}.$$

It follows that

$$\mathbb{E}_{X \sim \text{Unif}(d, R)} |J\Phi_d(X)|^{-1} \leq \int v^{-1} f_V(v) dv = C + \int_0^{R'} v^{-2} F_V(v) dv < \infty$$

as soon as $\tilde{d}\eta > 1$, which will happen for large enough d .

Let us thus prove (55) by induction on K . When $K = 1$, $V = |\det \bar{J}U(\bar{X}_1)| = |\bar{J}U(\bar{X}_1)|$ and assumption (C) directly implies that

$$F_V(y) = P(|Z| \leq y) \lesssim y^\eta.$$

Now, suppose (55) is true for $K - 1$ and let us prove it for K . We use the following lemma:

Lemma A.1. *We say that a bounded random vector Z in $B(K, R) \subset \mathbb{R}^K$ has property (*) if there exists $\eta > 0$ such that*

$$\forall S \subset \mathbb{R}^K \text{ Lebesgue measurable}, P(Z \in S) \lesssim |S|^\eta.$$

If Z has property () and $K > 1$, then Z_H , the orthogonal projection of Z onto any hyperplane, also has property (*), and*

$$\mathbb{E}(\|Z\|^{-\eta}) < C_{R, \eta}. \quad (56)$$

Before proving the lemma, let us conclude with (55). By denoting $Z_i = \bar{J}U(\bar{X}_i)$, $i = 1 \dots K$, and assuming $\|Z_1\| > 0$, one Gauss-Jordan iteration yields

$$\det [Z_1, \dots, Z_K] = \|Z_1\| \det [\tilde{Z}_2, \dots, \tilde{Z}_K] ,$$

where \tilde{Z}_i is the projection of Z_i onto the orthogonal complement of Z_1 . From lemma A.1, \tilde{Z}_i , $i = 2, \dots, K$ satisfies assumption (C), since we compute it with an orthogonal projection that depends only on Z_1 , which is independent from all the Z_i , $i \geq 2$. Thus by induction hypothesis and using (56) we obtain

$$\begin{aligned} F_Y(y) = P(|\det [Z_1, \dots, Z_K]| \leq y) &= P\left(\|Z_1\| |\det [\tilde{Z}_2, \dots, \tilde{Z}_K]| \leq y\right) \\ &= \mathbb{E}_{Z_1} P\left(|\det [\tilde{Z}_2, \dots, \tilde{Z}_K]| \leq y \|Z_1\|^{-1} \mid Z_1\right) \\ &\leq \mathbb{E}_{Z_1} y^\eta \|Z_1\|^{-\eta} \lesssim y^\eta , \end{aligned}$$

which proves (55).

Let us finally prove lemma A.1. Let S_H be a measurable set in a given hyperplane H of dimension $K - 1$, and let $\tilde{S} = S_H \times (-R, R)$ by the corresponding cylinder in $B(K, R)$. By definition, we have

$$P(Z_H \in S_H) = P(Z \in \tilde{S}) \leq |\tilde{S}|^\eta = |S_H|^\eta (2R)^\eta$$

which proves that Z_H also has the property (*).

Finally, let us show that $\mathbb{E}(\|Z\|^{-\eta}) < C_{R,\eta}$. For positive random variables we have

$$\begin{aligned} \mathbb{E}(\|Z\|^{-\eta}) &= \int_0^R r^{-\eta} f_{\|Z\|}(r) dr \\ &= R^\eta - \lim_{r \rightarrow 0} r^{-\eta} P(\|Z\| \leq r) + \eta \int_0^R r^{-\eta-1} P(\|Z\| \leq r) dr \\ &\leq R^\eta + C\eta \int_0^R r^{-\eta-1+\eta K} dr \leq C_{R,\eta} , \end{aligned}$$

since $K > 1$ and $\eta > 0$. This proves lemma A.1 and thus (26). \square

To prove that $\gamma_d(y)$ is integrable on any bounded set, we apply the coarea formula to (52) to $g(x) = |J_K \Phi x|^{-1} 1_A(\Phi x)$ where A is bounded:

$$\int_{\mathbb{R}^n} 1_A(\Phi x) dx = \int_A \int_{\Phi^{-1}(z)} |J_K \Phi x|^{-1} d\mathcal{H}^{d-K} dz = \int_A \gamma_d(z) dz .$$

If A is compact then $\sup_{x \in A} \|x\|_2 = R < \infty$. Since $\|\Phi x\|_2 \geq \kappa \beta \|x\|_2$ so

$$\int_B 1_A(\Phi x) dx \leq \int_B 1_{\|\Phi x\|_2 \leq R} dx \leq B \int 1_{\|x\|_2 \leq R \kappa^{-1} \beta^{-1}} dx = \frac{2\pi^d}{\Gamma(d+1/2)} R^{d-1} \kappa^{-d} \beta^{-d}, \quad (57)$$

which proves that γ_d is integrable on a compact.

A.2 Proof of part (ii)

Let us now prove that for each d , $\gamma_d(y)$ can only vanish when $\text{dist}(y, \overline{\Phi_d(\Omega_d)}) \leq c/d$ for some fixed constant c . We will exploit the relationship between the sets $\Phi_d(\Omega_d)$ and $\Phi_{d/2}(\Omega_{d/2})$ thanks to the fact that Φ_d is an average potential over the domain.

The inequality (27) proves that $\gamma_d(y) = 0$ only if $\int_{\Phi^{-1}(y)} d\mathcal{H}^{d-K} = 0$. Since in finite integer dimensions the Hausdorff measure \mathcal{H}^ℓ is a multiple of the Lebesgue measure in \mathbb{R}^ℓ , it is sufficient to show that whenever $y \in (\Phi_d(\Gamma_d))^\circ$, the set $\Phi^{-1}(y)$ has positive Lebesgue measure of dimension $d - K$.

Let us write $d = r^\ell$, with r denoting the length of the cube Λ_d . Suppose first that r is even. Without loss of generality, assume that $\Phi = (\phi_1, \dots, \phi_K)$ are linearly independent functions. Otherwise, if there were a linear dependency of the form

$$\sum_{k \leq K} \alpha_k \phi_k(x) \equiv 0$$

then $\Phi_d(\Omega_d) = \partial\Phi_d(\Omega_d)$ and the result is trivially true.

For that purpose, given $y \in (\Phi_{2^{-\ell}d}(\Omega_{2^{-\ell}d}))^\circ$ we will see that there exists $x \in \Phi^{-1}(y)$ whose Jacobian $J\Phi x$ has rank K . Then, by the Implicit Function Theorem, one can find a local reparametrization of $\Phi^{-1}(y)$ in a small neighborhood V of the form $x = (v, \varphi(v))$ such that

$$\{(v, \varphi(v)); v \in V \subset \mathbb{R}^{d-K}, \varphi : V \rightarrow \mathbb{R}^K\} = \{(v, v') \in V \times \varphi(V); \Phi(v, v') = y\},$$

which has positive Lebesgue measure of dimension $d - K$.

Suppose first that $\Delta = 1$. Then the sets $S_d = \Phi_d(\Omega_d) \subset \mathbb{R}^K$ satisfy $S_d \subseteq S_{q^\ell d}$ for $q = 1, 2, \dots$. Indeed, given $y \in S_d$, by definition there exists $x \in \Omega_d$ with $\Phi_d(x) = y$. Consider $\tilde{x} = (x, \dots, x)^{\otimes \ell} \in \Omega_{q^\ell d}$, a tiling of x , q times along each dimension. By construction, \tilde{x} satisfies $\Phi_{q^\ell d}(\tilde{x}) = y$ and therefore $y \in S_{q^\ell d}$.

Now, consider $y \in S_d^\circ \subseteq S_{2^\ell d}^\circ$. If Φ_d was a smooth C^∞ Lipschitz map, then by Sard's theorem, the image of critical points $\{x \in \Omega_d; |J\Phi_d(x)| < K\}$ has zero Lebesgue measure in S_d . In our setting, we will use a weaker property that does not require the smoothness assumption, as described in the following lemma:

Lemma A.2. *Under the assumptions of the theorem, the set $A = \{y \in \mathbb{R}^K; 0 < \gamma_d(y) < \infty\}$ is dense in $\Phi_d(\Omega_d)$, and for each $y \in A$ there exists $x \in \Phi_d^{-1}(y)$ with $|J\Phi_d(x)| > 0$.*

It follows that for a sufficiently small $\delta > 0$, a neighborhood $B(y, \delta) \subset S_d$ of y necessarily contains two points $y_1 = y + \eta$, $y_2 = y - \eta$ such that $\Phi_d^{-1}(y_1)$ or $\Phi_d^{-1}(y_2)$ contain a regular point. Let $x_1 \in \Phi_d^{-1}(y_1)$ and $x_2 \in \Phi_d^{-1}(y_2)$ be two points such that at least one is regular. The point $\tilde{x} = (x_1^{\otimes \ell}, x_2^{\otimes \ell}) \in \Omega_{2^\ell d}$, obtained by concatenating x_1 and x_2 along the first coordinate, and tiling them along the rest, satisfies

$$\Phi_{2^\ell d}(\tilde{x}) = \frac{1}{2} (\Phi_d(x_1) + \Phi_d(x_2)) = y, \text{ and}$$

$$|J\Phi_{2^\ell d}(\tilde{x})| \geq \max(|J\Phi_d(x_1)|, |J\Phi_d(x_2)|) > 0 ,$$

which shows that we have just found an element \tilde{x} of $\Phi_{2^\ell d}^{-1}(y)$ with $\text{rank}(J\Phi_{2^\ell d}(\tilde{x})) = K$.

Suppose finally that $\Delta > 1$. The proof follows the same strategy, but we need to handle the border effect introduced by the support Δ . In that case, given $y \in S_d$, we consider $\tilde{x} = (x, u, x)^{\otimes \ell}$, where u has $2(\Delta - 1)$ zero coordinates and $x \in \Phi_d^{-1}(y)$. That is, we consider 2^ℓ copies of x separated by $2(\Delta - 1)$ zeroes along each dimension so that their potential functions do not interact.

Let $\tilde{d} = (2r + 2(\Delta - 1))^\ell$. It follows that

$$\Phi_{\tilde{d}}(\tilde{x}) = \frac{2^\ell d \Phi_d(x)}{\tilde{d}} = \left(1 + \frac{\Delta - 1}{r}\right)^{-\ell} \Phi_d(x) = \left(1 + \frac{\Delta - 1}{d^{1/\ell}}\right)^{-\ell} y ,$$

which shows that $\text{dist}(y; S_{\tilde{d}}) \lesssim C\ell\|y\|/d^{1/\ell}$ for any $y \in S_d$.

Now consider y in the open set $C_d = S_d \cap S_{\tilde{d}}$, such that $\text{dist}(y, \partial S_d) \geq \|y\|\ell\Delta d^{-1/\ell}$. It follows from the previous argument that there exists small $\delta > 0$ and $x_1 \in \Phi_d^{-1}(y_1)$ with $|J\Phi_d(x_1)| > 0$ and $y_1 \in B(y, \delta) \cap S_d \cap S_{\tilde{d}}$. We verify from the assumption that

$$y_2 = 2 \left(1 + \frac{\Delta - 1}{r}\right)^\ell y - y_1 \in S_d ,$$

and therefore for any $x_2 \in \Phi_d^{-1}(y_2)$ the point $\tilde{x} = (x_1; u, x_2)^{\otimes \ell}$ that contains $2^{\ell-1}$ copies of x_1 and $2^{\ell-1}$ copies of x_2 satisfies by construction

$$\Phi(\tilde{x}) = \frac{d2^{\ell-1}y_1 + d2^{\ell-1}y_2}{\tilde{d}} = y \quad \text{and}$$

$\text{rank}(J\Phi_{2d}(\tilde{x})) = K$. Finally, the case where r is odd is treated analogously, but splitting the coordinates into $\lfloor \frac{r}{2} \rfloor$ and $\lceil \frac{r}{2} \rceil$ parts.

It remains to prove Lemma A.2. We know from part (i) that thanks to the coarea formula,

$$\forall \epsilon \forall y \in (\Phi_d(\Gamma_d))^\circ, \quad 0 < \int_{\|z-y\| \leq \epsilon} \gamma_d(z) dz = \int_{\|\Phi(x)-y\| \leq \epsilon} dx < \infty .$$

It follows that $A = \{z; 0 < \gamma_d(z) < \infty\}$ is dense in $\Phi_d(\Omega_d)$. But if $y \in A$, by definition this implies that $\Phi_d^{-1}(y)$ has positive $d-K$ -Hausdorff measure, and that there is necessarily $x \in \Phi_d^{-1}(y)$ with $|J\Phi_d(x)|^{-1} < \infty$, therefore with a full-rank Jacobian. \square

A.3 Proof of part (iii)

In order to prove (28), we will again exploit the relationships between the sets $S_d = \Phi_d(\Gamma_d)$ as d grows. We also first establish the result for $\Delta = 1$, and then generalize it to $\Delta > 1$.

Denote as before $S_d = \Phi_d(\Gamma_d)$ and $F_{d,\epsilon}^y = d^{-1}H(p_{d,\epsilon}^y)$ the entropy rate associated with y and ϵ .

In the last section we proved that when $\Delta = 1$, $S_d \subseteq S_{q^\ell d}$ for $q = 1, 2, \dots$. For any $\epsilon > 0$ and $y \in S_d$, observe that

$$\Phi_{d,\epsilon}^{-1}(y) \underbrace{\otimes \cdots \otimes}_{2^\ell \text{ times}} \Phi_{d,\epsilon}^{-1}(y) \subseteq \Phi_{2^\ell d,\epsilon}^{-1}(y) . \quad (58)$$

Indeed, if $x \in \Phi_{d,\epsilon}^{-1}(y) \underbrace{\otimes \cdots \otimes}_{2^\ell \text{ times}} \Phi_{d,\epsilon}^{-1}(y)$, then by definition $x = (x_1, \dots, x_{2^\ell})$ with

$$\|\Phi_d(x_i) - y\| \leq \epsilon .$$

But

$$\Phi_{2^\ell d}(x) = 2^{-\ell} \sum_{i=1}^{2^\ell} \Phi_d(x_i)$$

and $\|\Phi_{2^\ell d} - y\| \leq \epsilon$ by the convexity of the ℓ^2 norm, thus $x \in \Phi_{2^\ell d,\epsilon}^{-1}(y)$. It follows that

$$F_{2^\ell d,\epsilon}^y = d^{-1}H(p_{2^\ell d,\epsilon}^y) \geq d^{-1} \log \left([\gamma_{d,\epsilon}^y]^{2^\ell} \right) = F_{d,\epsilon}^y . \quad (59)$$

Thus, for any fixed d_0 , $y \in S_{d_0}$ and $\epsilon > 0$, the sequence $F_k = F_{2^{k\ell} d_0,\epsilon}^y$ is increasing. Also, thanks to assumption (B), we have that

$$\forall d , x \in \Phi_{d,\epsilon}^{-1}(y) \implies \|x\| \leq C(\|y\| + \epsilon) ,$$

which implies that $|\Phi_{d,\epsilon}^{-1}(y)| \leq |B_d(0, R_0)|$ where R_0 is independent of d . Therefore

$$\forall d , F_{d,\epsilon}^y \leq d^{-1} \log |B_d(0, R_0)| \leq \tilde{C}$$

which shows that the entropy rate F_k is also upper bounded, and therefore its limit exists $\lim_{k \rightarrow \infty} F_k = \bar{F}$. We shall see later that the limit does not depend upon the choice of d_0 .

Let us now prove the case when $\Delta > 1$. The idea is to show that (58) is now valid up to an error that becomes small as d increases, provided that the potential U is bounded.

Consider $y \in S_d$. Given $\epsilon > 0$, we form

$$\Psi_{2^\ell d,\epsilon}(y) = \left(\Phi_{d,\epsilon}^{-1}(y) \right)^{\otimes 2^\ell}$$

as the Cartesian product of 2^ℓ copies of $\Phi_{d,\epsilon}^{-1}(y)$. When $\Delta = 1$, we just saw that

$$\Psi_{2^\ell d,\epsilon}(y) \subseteq \Phi_{2^\ell d,\epsilon}^{-1}(y) \quad (60)$$

with $\epsilon = \tilde{\epsilon}$, but when $\Delta > 1$, let us see how to increase $\tilde{\epsilon}$ so that (60) is verified. Given $x \in \Psi_{2^\ell d, \epsilon}(y)$, we write $x = (x_1, \dots, x_{2^\ell})$ to denote its projections into each of the 2^ℓ subdomains $C_{1,d}, \dots, C_{2^\ell, d}$ of size d . We have

$$\begin{aligned}\Phi_{2^\ell d}(x) &= \frac{\sum_n Ux(n)}{2^\ell d} \\ &= 2^{-\ell} \sum_{k=1}^{2^\ell} d^{-1} \left(\sum_{n \in C_{k,d}^\circ} Ux(n) + \sum_{n \in \partial C_{k,d}} Ux(n) \right),\end{aligned}\tag{61}$$

where each $C_{k,d}^\circ$ contains the interior of the domain that does not interact with the other domains, and $\partial C_{k,d} = C_{k,d} \setminus C_{k,d}^\circ$. We have $|\partial C_{k,d}| = d - (d^{1/\ell} - 2\Delta)^\ell$, thus

$$d^{-1}|\partial C_{k,d}| = 1 - (1 - 2\Delta d^{-1/\ell})^\ell \lesssim \frac{\ell\Delta}{d^{1/\ell}}.\tag{62}$$

Since $|Ux(n)| \leq B$ by the boundedness assumption, it follows from (61) and (62) that

$$\begin{aligned}\|\Phi_{2^\ell d}(x) - y\| &= \left\| 2^{-\ell} \sum_{k=1}^{2^\ell} \left[d^{-1} \left(\sum_{n \in C_{k,d}^\circ} Ux(n) + \sum_{n \in \partial C_{k,d}} Ux(n) \right) - y \right] \right\| \\ &\leq 2^{-\ell} \sum_{k=1}^{2^\ell} \left(\|\Phi_d(x_i) - y\| + 2B(1 - (1 - 2\Delta d^{-1/\ell})^\ell) \right) \\ &\leq \epsilon + o\left(\frac{\ell\Delta}{d^{1/\ell}}\right),\end{aligned}$$

Thus by taking $\tilde{\epsilon} = \epsilon + o\left(\frac{\ell\Delta}{d^{1/\ell}}\right)$ (60) is verified. It follows that the entropy rate $F_{d,\epsilon}^y$ satisfies

$$F_{d,\epsilon}^y \leq F_{2^\ell d, \epsilon + \tilde{\ell} d^{-1}}^y,$$

with $\tilde{\ell} = C\Delta\ell$, which implies by repeating the inequality that for sufficiently large d and $k = 1, 2, \dots$ and $\epsilon > 0$ we have

$$F_{d,\epsilon}^y \leq F_{d2^{k\ell}, \epsilon + \tilde{\ell} d^{-1} \sum_{k'=0}^k 2^{-k'}}^y \leq F_{d2^{k\ell}, 2\epsilon}^y \leq \tilde{C},\tag{63}$$

and thus by defining

$$F_{\infty, \epsilon}^y := \lim_{k \rightarrow \infty} F_{d0 2^{k\ell}, \epsilon_k}^y, \text{ with } \epsilon_k = \epsilon + \tilde{\ell} d^{-1/\ell} \sum_{k'=0}^k 2^{-k'}$$

we have shown that its entropy rate is well-defined for each $\epsilon > 0$ and d_0 sufficiently large.

It remains to be shown that this limit does not depend upon d_0 . Suppose $F_{\infty,\epsilon,0} \neq F_{\infty,\epsilon,1}$ where F_0 is associated with d_0 and F_1 is associated with d_1 , and suppose $d_1 > d_0$ without loss of generality. Let $r_i = d_i^{1/\ell}$ for $i = 0, 1$.

Observe that an analogous argument to (61) shows that if $r = r_a + r_b$, then

$$F_{r^\ell, \tilde{\epsilon}} \geq \frac{r_a}{r} F_{r_a^\ell, \epsilon} + \frac{r_b}{r} F_{r_b^\ell, \epsilon} , \quad (64)$$

and

$$F_{l^\ell d, \tilde{\epsilon}} \geq F_{d, \epsilon} \text{ for } l = 1, 2, \dots , \quad (65)$$

with $\tilde{\epsilon} = \epsilon + o\left(\frac{\ell\Delta}{d^{1/\ell}}\right)$. Consider now large integers k and $\tilde{k} \simeq \sqrt{k}$, and let q, \tilde{q} denote respectively the quotient and residual such that

$$r_1 2^k = r_0 2^{\tilde{k}} q + \tilde{q}$$

with $0 \leq \tilde{q} < r_0 2^{\tilde{k}}$. Then, for any $\delta > 0$, by choosing k large enough we obtain from (64) and (65) that

$$\begin{aligned} |F_{d_1 2^{k\ell}, \tilde{\epsilon}} - F_1| &\leq \delta/4 , \\ |F_{d_0 2^{\ell\tilde{k}} q^\ell, \tilde{\epsilon}} - F_0| &\leq \delta/4 , \text{ and} \\ |F_{d_1 2^{k\ell}, \tilde{\epsilon}} - F_{d_0 2^{\ell\tilde{k}} q^\ell, \tilde{\epsilon}}| &\leq \delta/4 , \end{aligned} \quad (66)$$

with $\bar{\epsilon} = \tilde{\epsilon} + o\left(\frac{\ell\Delta}{d^{1/\ell}}\right)$.

Finally, let us show that $F_{d,\epsilon}^y$ is continuous with respect to ϵ for $\epsilon > 0$. Let us denote $\gamma_{d,\epsilon}^y = \int_{\|z-y\| \leq \epsilon} \gamma_d(z) dz$. Since $F_{d,\epsilon}^y = d^{-1} \log(\gamma_{d,\epsilon}^y)$ and $\gamma_d(y) > 0$ for all $y \in S_d^\circ$ from last section, it is sufficient to show that $\gamma_{d,\epsilon}^y$ is continuous with respect to ϵ . Let $\tilde{\epsilon} = \epsilon + \delta$ with $\epsilon > 0$, and suppose $\delta > 0$ without loss of generality. By denoting $Q(\delta, \epsilon, y) = \{z; \epsilon < \|z - y\| \leq \epsilon + \delta\}$, we have

$$\begin{aligned} |\gamma_{d,\tilde{\epsilon}}^y - \gamma_{d,\epsilon}^y| &= \int_{\epsilon < \|z-y\| \leq \epsilon+\delta} \gamma_d(z) dz = \int \gamma_d(z) \mathbf{1}_{Q(\delta, \epsilon, y)}(z) dz \\ &:= \int \gamma_{d\delta}(z) dz \end{aligned}$$

For each z , $\gamma_{d\delta}(z) = \gamma_d(z) \mathbf{1}_{Q(\delta, \epsilon, y)}(z)$ converges pointwise to 0 as $\delta \rightarrow 0$, except for a set of measure zero, $\{z; \|z - y\| = \epsilon\}$. Also, $|\gamma_{d\delta}| \leq \gamma_d$, which is integrable in $\Phi(\Omega_d)$ by part (i). We can thus apply the dominated convergence theorem, and conclude that

$$\lim_{\delta \rightarrow 0} \int \gamma_{d\delta}(z) dz = \int \left(\lim_{\delta \rightarrow 0} \gamma_{d\delta}(z) \right) dz = 0 ,$$

which shows that $\gamma_{d,\epsilon}^y$ is continuous with respect to ϵ .

It follows from (66) that

$$|F_{d_1 2^{k\ell}, \tilde{\epsilon}} - F_{d_0 2^{\tilde{k}\ell} q^\ell, \tilde{\epsilon}}| \rightarrow 0 \text{ as } k \rightarrow \infty ,$$

but $F_{d_1 2^{k\ell}, \tilde{\epsilon}} \rightarrow F_1$ and $F_{d_0 2^{\tilde{k}\ell} q^\ell, \tilde{\epsilon}} \rightarrow F_0$ as $k \rightarrow \infty$, which is a contradiction with the fact that $F_0 \neq F_1$. \square

B Proof of Proposition 3.2

Properties (A) and (B) are verified for (i-ii) because the potentials U are continuous and the resulting features Φ always include $d^{-1}\|x\|^2$ respectively. We thus focus on proving property (C).

Part (i) is easily obtained, since the \mathbf{I}^2 wavelet model has a Jacobian $J\Phi(x)$ that is linear with respect to x , and therefore it has absolutely continuous density relative to the Lebesgue measure.

Part (ii) is proved by directly controlling $|J\Phi_d(x)|^{-1}$. A direct computation shows that $|J\Phi_d(x)| = d^{-1}\sqrt{d\|x\|^2 - \|x\|_1^2}$, which only vanishes when $|x|$ is a constant vector. Therefore, for $y \neq (\alpha, \Lambda_d \alpha)$, $\Phi_{d,\epsilon}^{-1}(y)$ does not contain those points for sufficiently small ϵ .

Let us now show part (iii). The Jacobian matrix in that case is given by

$$J\Phi_d(x)_j = d^{-1} \text{Re} \left\{ \left(\frac{x \star h_j}{|x \star h_j|} \right) \star h_j^* \right\} ,$$

with $j \leq K$. We proceed by induction over the scale K . Suppose first $K = 1$. Since h_j has compact spatial support, its Fourier transform only contains a discrete number of zeros. Denote by Δ_j the spatial support of h_j . We can thus generate all but a zero-measure set of unitary signals z with $z_s = e^{i\theta_s}$, $s = 1 \dots \Delta_j$ from the uniform measure over x using $z = \frac{x \star h_j}{|x \star h_j|}$. In the uniform phase space defined by $\theta_1, \dots, \theta_{\Delta_j}$, the event $|\det \bar{J}U(\bar{X}_1)| \leq y$ has a probability proportional to y , since it is equivalent to

$$\left| \sum_s \cos(\theta_s) \text{Re}(h_j^*(s)) - \sum_s \sin(\theta_s) \text{Im}(h_j^*(s)) \right| \leq y .$$

Suppose now the result holds for the $K - 1$ filters in the family with smallest spatial support, and let us show how to extend it to an extra filter h_K with strictly larger spatial support. Among the variables $\bar{X} \in \mathbb{R}^{2\Delta+1}$, a subset of them, say R_K , only affect the K -th output corresponding to filter h_K . It follows that a set $S \subset \mathbb{R}^K$ with shrinking measure necessarily introduces constraints on the variables in R_K , and therefore $P(Z \in S) \leq |S|^{1/K}$. \square .

C Proof of Theorem 3.4

C.1 Proof of part (i)

We prove this result by induction on n . μ_0 is stationary by construction. Suppose now that μ_n is stationary. From (31), $\mu_{n+1} = \varphi_{n,\#}\mu_n$, with

$$\varphi_n(x) = x - \kappa_n J\Phi_d(x)^\top (\Phi_d(x) - y) .$$

Let $T_u x$ denote a (circular) shift of $x \in I^{\Lambda_d}$ by $u \in \Lambda_d$. Let us verify that φ_n is translation equivariant: $\varphi_n T_u x = T_u \varphi_n x$ for all x and u . Since Φ_d is translation invariant, $\Phi_d T_u x = \Phi_d x$, and since T_u is linear,

$$J\Phi_d(x) = J(\Phi_d \circ T_u)(x) = J\Phi_d(T_u x) T_u ,$$

thus

$$J\Phi_d(T_u x)^\top = T_u (J\Phi_d(x))^\top \quad (67)$$

since $T_u^\top = T_{-u}$ and $T_u \circ T_{-u} = \mathbf{1}$. It follows from (67) that

$$\begin{aligned} \varphi_n T_u x &= T_u x - \kappa_n J\Phi_d(T_u x)^\top (\Phi_d(T_u x) - y) \\ &= T_u x - T_u \kappa_n J\Phi_d(x)^\top (\Phi_d(x) - y) \\ &= T_u \varphi_n x , \end{aligned}$$

which proves that φ_n is translation equivariant. Moreover, we verify that if φ is a diffeomorphism that is translation equivariant, then φ^{-1} is also translation equivariant. Indeed, let $x_u^a = \varphi^{-1}(T_u x)$ and $x_u^b = T_u \varphi^{-1}(x)$. We have

$$(T_{-u} \circ \varphi)(x_u^a) = x = (\varphi \circ T_{-u})(x_u^b) ,$$

but since $T_{-u} \circ \varphi \equiv \varphi \circ T_{-u}$ and it is a diffeomorphism, hence injective, it follows that necessarily $x_u^a = x_u^b$ for all x and u .

Finally, using the definition of pushforward measure, $\mu_{n+1} = \varphi_{n,\#}\mu_n$, for any measurable A , the induction hypothesis yields

$$\begin{aligned} \mu_{n+1}[T_u A] &= \mu_n[\varphi_n^{-1}(T_u A)] \\ &= \mu_n[T_u \varphi_n^{-1}(A)] = \mu_n[\varphi_n^{-1}(A)] \\ &= \mu_{n+1}[A] , \end{aligned}$$

which shows that μ_{n+1} is also stationary \square .

C.2 Proof of part (ii)

Let us first show how the strict saddle condition (32) implies that the minimisation $\mathcal{E}_y(x)$ has no poor local minima. The statement follows directly from [25], which show that when the saddle points are strict, gradient descent does not converge to those saddle points, up to a set of initialization values with Lebesgue measure 0.

Observe that a critical point x such that $\nabla \mathcal{E}_y(x) = J\Phi_d(x)^T(\Phi_d(x) - y) = 0$ necessarily falls into two categories. Either $\Phi_d(x) = y$, which implies that x is a global optimum, either x is such that $J\Phi_d(x)^T v = 0$ with $v = \Phi_d(x) - y \neq 0$. We verify that assumption (32) implies that in that case x is a strict saddle point by observing that the Hessian of \mathcal{E}_y satisfies

$$\nabla^2 \mathcal{E}_y(x) = \sum_{k=1}^K \nabla^2 \Phi_k(x) v_k + J\Phi(x)^T J\Phi(x) .$$

Since μ_0 is absolutely continuous with respect to the Lebesgue measure, we can apply Theorem 2.1 from [29], and establish that gradient descent does not converge to any saddle point with probability 1.

Let us now prove that the hypothesis that $|J\Phi_d(x)| > 0$ for $x \in \Phi_d^{-1}(y)$ with $y \in \Phi_N N(I^{\Lambda_d})^\circ$, together with the strict saddle condition, implies that the gradient descent sequence x_n has a limit $\lim_{n \rightarrow \infty} x_n$ (that may depend upon x_0). For that, we will apply the following result from [1]:

Theorem C.1. *If $\mathcal{E}(x)$ is twice differentiable, has compact sub-level sets, and the Hessian $\nabla^2 \mathcal{E}(x)$ is non-degenerate on the normal space to the level set of local minimisers, then $\lim_{n \rightarrow \infty} x_n = x_\infty$.*

Indeed, since Φ_d satisfies assumption (B), it follows that the sublevel sets of \mathcal{E}_y , $\{x; \mathcal{E}_y(x) \leq t\}$ are compact for each t . We need to show that the Hessian of \mathcal{E}_y is non-degenerate on the normal space of $\Phi_d^{-1}(y)$. Since $\gamma_d > 0$ for $y \in \Phi_d(I^{\Lambda_d})^\circ$ for sufficiently large d from Theorem 3.1, $\Phi_d^{-1}(y)$ has positive $d - K$ -dimensional Hausdorff measure, hence it is sufficient to show that $\nabla^2 \mathcal{E}_y(x)$ has K strictly positive eigenvalues when $x \in \Phi^{-1}(y)$. But by definition,

$$\nabla^2 \mathcal{E}_y(x) = \sum_{k \leq K} \nabla^2 \phi_k(x)(\phi_k(x) - y_k) + J\Phi_d(x)^T J\Phi_d(x) ,$$

thus

$$\nabla^2 \mathcal{E}_y(x) = J\Phi_d(x)^T J\Phi_d(x) \quad \text{for } x \in \Phi_d^{-1}(y) . \quad (68)$$

Therefore, if $|J\Phi_d(x)| > 0$ for $x \in \Phi_d^{-1}(y)$, we can apply Theorem C.1, and conclude that the iterates x_n from the gradient flow have a limit, for each $x_0 \sim \mu_0$.

We have just proved that

$$\Pr_{\mu_0} \{(x_n)_n \text{ is Cauchy}\} = 1 ,$$

or, equivalently, that $X_n \sim \mu_n$ is almost surely Cauchy, which implies [31] that μ_n converges almost surely to a certain measure μ_∞ . Moreover, since $\lim_{n \rightarrow \infty} \|\nabla \mathcal{E}_y(x_n)\| = 0$, the strict saddle condition implies that x_n does not converge to saddle points, so we conclude that necessarily

$$\mu_\infty [\Phi_d^{-1}(y)] = \Pr_{\mu_0} \left\{ \lim_{n \rightarrow \infty} x_n \in \Phi_d^{-1}(y) \right\} = 1 ,$$

therefore that μ_∞ is supported in the microcanonical ensemble $\Phi_d^{-1}(y)$, which finishes the proof. \square

C.3 Proof of part (iii)

We first compute how the entropy is modified at each gradient step. By definition of the pushforward measure, for any diffeomorphism φ and any measurable g

$$\mathbb{E}_{x \sim \varphi_\# \mu} g(x) = \mathbb{E}_{x \sim \mu} g(\varphi(x)) .$$

Also, from a change of variables we have, by denoting $\tilde{\mu} = \varphi_\# \mu$, $\tilde{\mu}(x) = |J\varphi^{-1}(x)|\mu(\varphi^{-1}(x))$, and thus

$$\log \tilde{\mu}(x) = \log \mu(\varphi^{-1}(x)) - \log |J\varphi(\varphi^{-1}(x))| .$$

It follows that

$$-\mathbb{E}_{x \sim \tilde{\mu}} \log \tilde{\mu}(x) = -\mathbb{E}_{x \sim \mu} \log \mu(x) + \mathbb{E}_{x \sim \mu} \log |J\varphi(x)|$$

and hence

$$H(\varphi_\# \mu) = H(\mu) - \mathbb{E}_\mu \log |J\varphi(x)| . \quad (69)$$

The change in entropy by applying the diffeomorphism is thus given by the term $\mathbb{E}_\mu \log |J\varphi(x)|$, and thus the entropy of μ_n is given by

$$H(\mu_n) = H(\mu_0) - \sum_{n' \leq n} \mathbb{E}_{\mu_{n'}} \log |J\varphi_{n'}(x)|$$

By definition, the Jacobian of φ_n is

$$J\varphi_n(x) = \mathbf{1} - \gamma_n \left(\sum_{k \leq K} \nabla^2 \phi_k(x) (\phi_k(x) - y_k) + J\Phi_d(x)^T J\Phi_d(x) \right) . \quad (70)$$

We know that Φ is Lipschitz, which implies that $\|J\Phi(x)\| \leq \beta$, and that $\nabla \Phi$ is also Lipschitz, meaning that $\|\nabla^2 \Phi_k(x)\| \leq \eta$ for all k . Applying Cauchy-Schwartz, it follows that

$$\left\| \sum_{k \leq K} \nabla^2 \Phi_k(x) (\Phi_k(x) - y_k) \right\| \leq \eta K \sqrt{E_y(x)} .$$

We abuse notation and redefine $\eta := \eta K$ since K is a constant. Also, the term $J\Phi(x)^T J\Phi(x)$ is of rank at most K . We can thus write $J\varphi_n(x)$ as

$$J\varphi_n(x) = A_n(x) + B_n(x) , \quad (71)$$

with $A_n(x)$ full rank d and with singular values within the interval $(1 - \gamma_n \eta \sqrt{E_y(x)}, 1 + \gamma_n \eta \sqrt{E_y(x)})$; and $-B_n(x)$ positive semidefinite of rank K , with singular values bounded by $\gamma_n \beta^2$. It results that the singular values of $J\varphi_n(x)$ $\lambda_1, \dots, \lambda_d$ satisfy

$$\begin{aligned} |\log |J\varphi_n(x)|| &\leq \sum_{i=1}^d |\log \lambda_i| \\ &\leq \sum_{i=1}^{d-K} \max(|\log(1 + \gamma_n \eta \sqrt{E_y(x)})|, |\log(1 - \gamma_n \eta \sqrt{E_y(x)})|) \\ &\quad + \sum_{i=1}^K |\log(1 - \gamma_n \beta^2)| \\ &\leq (d - K) \log(1 + \gamma_n \eta \sqrt{E_y(x)}) + K \log(1 + \gamma_n \beta^2) + o(\gamma_n^2) \end{aligned}$$

and thus up to second order terms we have

$$\begin{aligned} \mathbb{E}_{\mu_n} \log |J\varphi_n(x)| &\leq (d - K) \log \left(1 + \gamma_n \eta \mathbb{E}_{\mu_n} \sqrt{E_y(x)} \right) + K \log(1 + \gamma_n \beta^2) , \\ &\leq (d - K) \gamma_n \eta \mathbb{E}_{\mu_n} \sqrt{E_y(x)} + K \gamma_n \beta^2 , \end{aligned} \quad (72)$$

where we have used Jensen's inequality on the concave function $\mathbb{E} \log(1 + X) \leq \log(1 + \mathbb{E} X)$ and $\log(1 + x) \leq x$ for $x \geq 0$. Denoting by $r_n = \mathbb{E}_{\mu_n} \sqrt{E_y(x)}$ the average distance to the microcanonical ensemble at iteration n , it results from (72) that after n steps of gradient descent the entropy rate has decreased at most

$$\left(1 - \frac{K}{d}\right) \eta \sum_{n' \leq n} \gamma_{n'} r_{n'} + \frac{K}{d} \beta^2 \sum_{n' \leq n} \gamma_{n'} .$$

D Proof of Corollary 3.5

The proof is a direct application of Theorem 3.4 and Sard's theorem, that states that if Φ_d is a \mathbf{C}^∞ Lipschitz function, then the image of its critical points $\{x ; |J\Phi_d(x)| = 0\}$ has zero measure. We can thus apply Theorem C.1 from part (ii) of the proof of Theorem 3.4 for almost every y \square .

E Proof of Theorem 3.6

We show that $\Phi_d(x) = \{d^{-1}\|x \star h_k\|_2^2\}_k$ satisfies the strict saddle condition.

The gradient of the loss function $\mathcal{E}(x) = \frac{1}{2}\|\Phi(x) - y\|^2$ is

$$\nabla \mathcal{E}(x) = J\Phi_d(x)^T(\Phi_d(x) - y) ,$$

and its Hessian is

$$\nabla^2 \mathcal{E}(x) = \sum_k \nabla^2 \phi_k(x) v_k + J\Phi_d(x)^\top J\Phi_d(x) ,$$

where $v_k = \phi_k(x) - y_k$. Expressing the gradient and the Hessian in the Fourier domain yields

$$\nabla \mathcal{E}(\hat{x}) = \hat{x} \cdot \left(\sum_k v_k |\hat{h}_k|^2 \right) \quad (73)$$

$$\nabla^2 \mathcal{E}(\hat{x})(\omega, \omega') = \sum_k v_k |\hat{h}_k(\omega)|^2 \delta(\omega - \omega') + \hat{x}(\omega) |\hat{h}_k(\omega)|^2 \hat{x}(\omega')^* |\hat{h}_k(\omega')|^2 . \quad (74)$$

The Hessian thus contains a diagonal term and a rank- K term. We need to show that a critical point x satisfying $\nabla \mathcal{E}(\hat{x}) = 0$ with $\|v\| > 0$ has a Hessian matrix with at least one negative eigenvalue. From (73), it follows that a critical point satisfies

$$\forall \omega , \quad \hat{x}(\omega) \cdot \left(\sum_k v_k |\hat{h}_k(\omega)|^2 \right) = 0 . \quad (75)$$

Let $C = \{\omega ; \hat{x}(\omega) \neq 0\}$. The Hessian is expressed in terms of block matrices regrouping the frequencies in C as

$$\nabla^2 \mathcal{E}(\hat{x}) = \left(\begin{array}{c|c} \text{diag}(\sum_k v_k |\hat{h}_k(\omega)|^2) & 0 \\ \hline 0 & \nabla_{C,C}^2 \end{array} \right) .$$

We examine the diagonal block corresponding to the frequencies outside C , such that $\hat{x}(\omega) = 0$. The image of Φ_d is the convex cone \mathcal{C} in \mathbb{R}_+^K determined by the directions $o_\omega = (|\hat{h}_1(\omega)|^2, \dots, |\hat{h}_K(\omega)|^2) \in \mathbb{R}^K$, $\omega = 1 \dots d$. Without loss of generality, we assume here that $\|o_\omega\| > 0$ for all ω , since frequencies that are invisible to all the filters do not play any role in the gradient descent. The target y is by hypothesis in the interior of \mathcal{C} . Further, any two directions o, o' in \mathcal{C} satisfy

$$\langle o, o' \rangle = \sum_k |\hat{h}_k(\omega)|^2 |\hat{h}_k(\omega')|^2 > 0 ,$$

since the filters have compact spatial support.

If $|C| = 0$, then $x = 0$, which implies that $v = \Phi(x) - y = -y$ has all its entries negative, and therefore $\text{diag}(\sum_k v_k |\hat{h}_k(\omega)|^2) < 0$. We shall thus assume in the following that $|C| > 0$.

Similarly, we verify that the space spanned by o_j , $j \in C$, cannot have full rank K . Indeed, if that were the case, the first order optimality condition (75) reveals that v should be orthogonal to all directions o_j , $j \in C$. Since this system has rank K , this contradicts the fact that $v \neq 0$.

Suppose then that some $j \in C$ is such that o_j is in the convex hull of \mathcal{C} . Since $\text{rank}(\{o_j ; j \in C\}) < K$, there exists another direction in the convex hull of \mathcal{C} that is not in C , say o_0 . Denoting by $u = \Phi_d(x)$, the orthogonal projection of \mathcal{C} into the subspace U spanned by u and o_0 is also a cone, which also satisfies $0 < \langle o_0, u \rangle < 1$. By abusing notation, we still denote by y the orthogonal projection of the original y to U , which is in the interior of \mathcal{C} . The first order optimality condition requires that

$$\langle \Phi_d(x), u \rangle = \langle y, u \rangle ,$$

but this condition necessarily implies that

$$\langle \Phi_d(x), o_0 \rangle < \langle y, o_0 \rangle ,$$

which shows that in this case there is at least one strictly negative eigenvalue.

Suppose finally that all the $j \in C$ are such that o_j is strictly inside the cone \mathcal{C} . Let us see that the sets

$$A = \{v; \langle v, o \rangle \geq 0 \ \forall \ o \in \mathcal{C}\} \text{ and } B(o) = \{v; \langle v, o \rangle = 0\} , o \in \mathcal{C}^\circ$$

satisfy

$$A \cap B(o) = \{0\} . \tag{76}$$

From (76), and since o_j , $j \in C$ is strictly inside the cone and $\|v\| > 0$ with $\langle v, o_j \rangle = 0$, it follows that $v \in B(o)$ and therefore v cannot belong to A , which implies that some direction o_i in the convex hull of \mathcal{C} must satisfy $\langle v, o_j \rangle < 0$, again implying the existence of a negative eigenvalue.

So let us finally prove (76). Since $o \in \mathcal{C}^\circ$, by denoting o_1, \dots, o_K the directions determining the convex hull of \mathcal{C} we have

$$o = \sum_k \alpha_k o_k , \text{ with } \alpha_k > 0 \ \forall \ k .$$

Pick any $v \in B(o)$. Then

$$0 = \langle v, o \rangle = \langle v, \sum_k \alpha_k o_k \rangle = \sum_k \alpha_k \langle v, o_k \rangle ,$$

and since any $v \in A$ must satisfy $\langle v, o_k \rangle \geq 0$ for all k , it follows that $\langle v, o_k \rangle = 0$ for all k is the only valid intersection, which corresponds to $v = 0$ since $\{o_k\}$ have full rank.

Finally, if $x \in \Phi_d^{-1}(y)$ for $y \in \Phi_d(I^{\Lambda_d})^\circ$, then y falls necessarily inside the convex hull of \mathcal{C} , which implies that $\{\nabla \phi_k(x) = \hat{x}(\omega) \cdot |\hat{h}_k|^2(\omega)\}_{k \leq K}$ have rank K . This concludes the proof \square .

F Proof of Theorem 4.1

Young inequality is proved by observing that

$$\|x \star \psi_{j,q}\|_1 = \sum_{n \in \Lambda_d} \left| \sum_{u \in \Lambda_d} x(u) \psi_{j,q}(n-u) \right| \geq \sum_{n \in \Lambda_d} \sum_{u \in \Lambda_d} |x(u) \psi_{j,q}(n-u)| = \|x\|_1 \|\psi_{j,q}\|_1 .$$

The inequality is an equality if and only if for any fixed n , the product $x(u) \psi_{j,q}(n-u)$ has a constant phase when u varies. Since $x(u)$ is real, its phase is either 0 or π . It implies that $\psi_{j,q}(n-u)$ has a phase modulo π which does not depend upon u when $x(u) \psi_{j,q}(n-u) \neq 0$. The phase of $\psi_{j,q}(u) = 2^{-\ell j} \psi_q(2^{-j}u)$ is $\varphi_q(2^{-j}u)$ so

$$\forall u \in \Lambda_d \quad , \quad \varphi_q(2^{-j}(n-u)) = a(2^{-j}n) + k\pi \quad \text{if } x(u) \psi_{j,q}(n-u) \neq 0 \text{ with } k \in \mathbb{Z} . \quad (77)$$

The theorem supposes that

$$\beta^{-1} |\omega_{q \cdot}(u-u')| \leq |\varphi_q(u) - \varphi_q(u')| \leq \beta |\omega_{q \cdot}(u-u')| . \quad (78)$$

If $2^{-j}|u-u'| \leq 2\alpha$ then for $n = (u+u')/2$ we have $2^{-j}|n-u| \leq \alpha$ and $2^{-j}|n-u'| \leq \alpha$, so $\psi_{j,q}(n-u) \neq 0$ and $\psi_{j,q}(n-u') \neq 0$. If the inner product $\omega_{q \cdot}(u-u')$ is not zero then (78) implies that $|\varphi_q(2^{-j}(n-u)) - \varphi_q(2^{-j}(n-u'))| > 0$. So if $x(u)$ and $x(u')$ are non-zero (77) implies that

$$|\varphi_q(2^{-j}(n-u)) - \varphi_q(2^{-j}(n-u'))| \geq \pi .$$

It results from (78) that if $2^{-j}|u-u'| \leq 2\alpha$ then

$$2^{-j} \beta |\omega_{q \cdot}(u-u')| \geq \pi ,$$

which proves (46). \square